The path to "femmes fatales": the evolution of toxin resistance in predatory fireflies.

Lu Yang[1], Flora Borne[2], Matthew L. Aardema[1,3], Ying Zhen[1,4], Julie Peng[1], Mariana Wu[1], Regina Visconti[1], Anja Betz[5], Bartholomew P. Roland[6,7], Aaron D. Talsma[6,7], Mike J. Palladino[6,7], Georg Petschenka[5], and Peter Andolfatto[2,*]

[1] Department of Ecology and Evolutionary Biology, Princeton University, Princeton, USA

[2] Department of Biological Sciences, Columbia University, New York, USA.

[3] Department of Biology, Montclair State University, Montclair, USA.

[4] School of Life Sciences, Westlake University, Hangzhou, China.

[5] Department of Applied Entomology, University of Hohenheim, Stuttgart, Germany

[6] Department of Pharmacology and Chemical Biology, University of Pittsburgh, Pittsburgh, USA

[7] Pittsburgh Institute for Neurodegenerative Diseases, University of Pittsburgh School of Medicine, Pittsburgh, USA

* Lead contact: pa2543@columbia.edu

Twitter: @pandolfatto

Summary:

Toxic cardiotonic steroids (CTS) act as a defense mechanism in many firefly species (Lampyridae) by inhibiting a crucial enzyme called Na^+,K^+-ATPase (NKA). While most fireflies produce these toxins internally, species of the genus *Photuris* acquire them from a surprising source: predation on other fireflies. The contrasting physiology of toxin metabolism between *Photuris* and other firefly genera suggests the possibility of distinct strategies evolving to prevent self-intoxication. Our study demonstrates that both *Photuris* and their firefly prey have evolved highly-resistant NKAs. Using an evolutionary analysis of the specific target of CTS (ATPα) in fireflies, and gene-editing in *Drosophila*, we find that the initial steps towards resistance were shared among *Photuris* and other firefly lineages. However, the *Photuris* lineage subsequently underwent multiple rounds of gene duplication and neofunctionalization, resulting in the development of ATPα paralogs that are differentially expressed and exhibit increasing resistance to CTS. In contrast, other firefly species have maintained a single copy. Our results implicate gene duplication as a facilitator in the transition of *Photuris* to its distinct ecological role as predator of toxic firefly prey.

.

One-Sentence Summary: Gene duplication is associated with distinct ecological roles for predatory fireflies and their firefly prey.

Introduction

Many species of fireflies (Lampyridae) produce a class of defensive toxins called cardiotonic steroids (CTS) that they use to deter potential predators (Berger et al. 2021; Gronquist et al. 2005; Meinwald et al. 1979; Smedley et al. 2017; Eisner et al. 1978; Tyler et al. 2008). In contrast, fireflies in the genus *Photuris* cannot manufacture their own CTS. Instead, they acquire these toxins by preying on other CTS-producing firefly species, using them as a defense for both themselves and their eggs (**Figure 1A**) (Lloyd 1965; Eisner et al. 1997; González et al. 1999a). Although most Lampyridae are predatory to varying degrees, only *Photuris* is documented to frequently prey on other fireflies. Among other adaptations associated with this specialization (Souto et al. 2019), female *Photuris* mimic the courtship signals of other female Lampyridae (including congeners) to attract male prey, earning them the moniker "*femmes fatales*" (Lloyd 1965; Lewis and Cratsley 2008).

CTS act by inhibiting Na^+,K^+-ATPase (NKA), an essential enzyme that helps maintain homeostasis in animals (Blanco and Mercer 1998; Lingrel 2009). CTS-resistant forms of NKA have evolved repeatedly across diverse insects and vertebrates via amino acid substitutions to the CTS-binding domain of the enzyme's alpha-subunit (ATPα, more specifically ATPα1) (Dobler et al. 2012; Holzinger and Wink 1996; Mohammadi et al. 2021, 2022; Moore et al. 2009; Petschenka et al. 2017; Ujvari et al. 2015; Yang et al. 2019; Zhen et al. 2012). CTS-adaptation in insects exhibits two distinct recurrent patterns of ATPα molecular evolution. The first is that CTS resistance typically evolves via a small number of amino acid changes, and most frequently via substitutions to three sites (111, 119 and 122) in the first extracellular domain (H1-H2) of the protein (Holzinger and Wink 1996; Zhen et al. 2012; Karageorgi et al. 2019; Taverner et al. 2019; Dobler et al. 2012). A second recurrent pattern in CTS-adapted insects is the frequent duplication and neofunctionalization of ATPα, with resistant and sensitive paralogs differentially allocated to the gut and nervous tissue (Yang et al. 2019; Zhen et al. 2012; Dobler et al. 2019). These findings generally point to a high degree of predictability in the genetic basis of CTS resistance evolution in insects (Zhen et al. 2012; Yang et al. 2019).

Here, we investigate whether ATPα1 is also a target of CTS-adaptation in fireflies and whether these adaptations evolved via similar mechanisms in firefly predators (i.e. *Photuris*) and other

firefly lineages. *Photuris* species share a number of adaptations with other fireflies including warning coloration and bioluminescent signaling (with associated structures). Collectively, these similarities likely reflect a combination of shared history and convergent evolution (Fallon et al. 2018; Oba et al. 2020; Branham and Wenzel 2003; Lloyd 1973). Accordingly, it is also possible that CTS resistance in *Photuris* and other firefly species evolved either in their common ancestor or convergently via similar molecular mechanisms. Alternatively, given the different physiological challenges associated with sequestering these toxins from a food source (i.e. *Photuris*) versus producing CTS autogenously (i.e. most other firefly species) (González et al. 1999; Heckel 2014; Petschenka and Agrawal 2016), it is also possible that distinct modes of CTS resistance evolved independently in *Photuris* and other firefly lineages.

Results

Duplication and neofunctionalization of ATPα1 in Photuris.

To investigate the basis of CTS resistance in predator and prey firefly species, we first considered the level of CTS resistance of membrane-bound NKA proteins isolated from the nervous systems of wild-caught *Photinus pyralis* (a representative prey species) and *Photuris versicolor* (a representative predator species). The enzymes of both species exhibit substantial levels of resistance to ouabain, a water-soluble form of CTS (**Figure 1B**, **Table S4**). While the monophasic inhibition curve for *Photinus* suggests a single resistant form of the enzyme, the curve for *Photuris* is still only partially inhibited at the highest inhibitor concentrations. We hypothesized that the curve is likely to be a truncated biphasic (or multi-phasic) curve, and that *Photuris* may have multiple isoforms of NKA that differ in their level of CTS resistance.

Using RNA-seq *de novo* assembly, we reconstructed ATPα1 sequences for multiple *Photuris* and other firefly species. Consistent with our *in vitro* CTS-inhibition assays (above), we found that *Photinus* and other toxin producing genera appear to have a single copy of ATPα1. In contrast, both *Photuris* species surveyed harbor multiple copies of ATPα1 that we designate as paralogs A-D (**Figure 2A**). Duplications of ATPα1 are absent in *Bicellonycha*, the immediate outgroup to the *Photuris* genus, indicating that all three duplication events occurred after the split of *Photuris*

and *Bicellonycha* (~50 Mya, (Höhna et al. 2022)), but prior to the split between *P. versicolor* and *P. frontalis*.

Photuris ATPα1 paralogs are differentially expressed among tissues. Based on the pattern of amino acid substitution at sites previously implicated in CTS-resistance, ATPα1A is predicted to be the most CTS-sensitive paralog and is more highly-expressed in head relative to gut tissue (adjusted p=3.0e-6). Conversely, ATPα1C and ATPα1D are predicted to be the most CTS-resistant paralogs because they have accumulated multiple amino acid substitutions implicated in CTS resistance (**Figure 2A-B**). In contrast to ATPα1A, ATPα1C is substantially more highly expressed in the gut relative to the head (adjusted p = 8.8e-4, **Table S2**, **Figure 2C**). This implies that ATPα1 paralogs have neofunctionalized, as observed in multiple CTS-adapted insects carrying ATPα1 duplications (Yang et al. 2019; Zhen et al. 2012; Dobler et al. 2019). ATPα1A and ATPα1C together comprise 88% of ATPα1 transcripts in the female *Photuris* head and are represented in roughly equal proportions (**Figure 2C**), lending support to the "biphasic" interpretation of the enzyme-inhibition curve for *Photuris* nervous tissue (**Figure 1B**). Given the stepwise accumulation of amino acid substitutions among *Photuris* paralogs (**Figure 2B**), we used CRISPR-Cas9 genome-editing (see Methods), and a similar site-directed cassette exchange system (Taverner et al. 2019), to generate a series of *Drosophila melanogaster* strains that carry substitutions occurring at key stages of ATPα1 neofunctionalization in *Photuris* (**Figure 3A**).

Phylogenetic inference reveals that the first steps in the evolution of ATPα1 CTS-resistance were shared between *Photuris* and other firefly lineages. Specifically, the substitution of alanine to valine at position 119 (A119V) likely preceded the split of *Photuris* and other fireflies (**Figure 2B**; **Supplementary Figure S1**). A subsequent substitution to the same site, V119I, is also observed in both *Photuris* and other firefly species. As *Bicellonycha* is neither a predator of other fireflies nor associated with CTS, this implies that V119I most likely evolved convergently in both *Photuris* and other firefly species after they became distinct lineages. This implies that V119I most likely evolved convergently in both *Photuris* and other firefly species soon after they became distinct lineages. To estimate the functional effects of the eventual transition from alanine to isoleucine at position 119 in *Photuris* and other firefly lineages, we modified the *D. melanogaster* ATPα1 protein using genome-editing tools. We find that A119I modestly but

significantly increases CTS resistance of NKA relative to the sensitive wild-type *D. melanogaster* enzyme (1.8-fold, 95% CI: 1.6-1.9; **Figure 3B**). A119I also substantially improves *D. melanogaster* adult survival upon exposure to CTS (**Figure 3C**). Since NKA is critical for proper neural function, we subjected adult engineered flies to mechanical over-stimulation and measured recovery time from induced seizures (the so-called "bang sensitivity" assay, ref. (Ganetzky and Wu 1982), see Methods). We found A119I mutant flies exhibit no obvious neurological dysfunction compared to wild-type flies (**Figure 3B**). Taken together, we conclude that the evolution of alanine to isoleucine at position 119 comprises a potential exaptation that may have facilitated the emergence of both the ability of fireflies to manufacture CTS and the predatory specialization of *Photuris*.

Despite these shared early steps in the evolution ATPα1 CTS-resistance, it is apparent that lineages leading to the predatory genus *Photuris* subsequently took a radically different approach compared to other fireflies: repeated duplication and neofunctionlisation of ATPα1. Following an initial duplication of ATPα1 in the *Photuris* lineage, two paralogous lineages began to diverge in function, with one lineage ancestral to more resistant paralogs B-D. The most conspicuous candidate CTS resistance substitutions on the B-D lineage are Q111E and T797I (**Figure 2B**). Site 111 is a known hotspot for convergent CTS resistance substitutions in animals (Dobler et al. 2012; Mohammadi et al. 2022; Zhen et al. 2012). At site 797, the ancestral threonine residue is predicted to form a stabilizing hydrogen bond between ATPα1 and CTS (Laursen et al. 2015) that the derived T797I substitution (along the paralog B-D lineage) is predicted to disrupt. Previous work established that the biochemically similar substitution T797V results in an 80-fold increase in CTS resistance of mammalian NKA (Feng and Lingrel 1994). A substitution to a third site in the paralog B-D lineage, A112S, was also of interest as this site was previously identified as a target of positive selection in CTS-resistant toads and their predators (Moore et al. 2009). Further, A112S repeatedly co-occurs with Q111E/R/T across phylogenetically diverse taxa including both insects and vertebrates (Mohammadi et al. 2022; Taverner et al. 2019).

Given these substitution patterns, we engineered a series of *D. melanogaster* lines to dissect the basis for CTS resistance along the lineage leading to paralogs B-D. We began by focusing on substitutions at sites 111 and 112. NKA isolated from fly lines engineered with Q111E+A112S

(hereafter "ES") exhibits a 6-fold increase in CTS resistance relative to the wild-type enzyme of fruit flies (**Figure 3B**; **Table S4**). Together, these substitutions also confer engineered adult flies with substantial levels of resistance to CTS exposure (**Figure 3C**, **Table S4**). Q111E and A112S each have significant effects individually (both ~2-fold) and their combined effects appear to be close to additive (**Supplementary Figure S4**; **Table S4**). We also find that the substitutions Q111E and A112S cause slight neural dysfunction when introduced individually, and this dysfunction is exaggerated when they are combined (in "ES" flies, **Figure 3D**, **Supplementary Figure S4**). These results suggest that the substantial CTS resistance conferred by this combination is associated with negative pleiotropic effects that may be compensated by other substitutions in ATP1α1 paralogs B-D.

While we did not generate lines representing the full complement of evolutionary paths along the paralogs B-D lineage, we find that substitution of T797I is homozygous lethal on the *D. melanogaster* ATP1α1 background. This is not unexpected given previous work showing that the similar substitution, T797V, decreases NKA activity to 3.4% of wild-type levels (Feng and Lingrel 1994). Interestingly, the isoleucine at site 797 of *Photuris* ATPα1B was replaced with valine after a second round of duplication (i.e. I797V, **Figure 2B**). Additional engineering reveals that the combination Q111E+A112S+A119I+D120A (hereafter "ESIA"), occurring along the ATPα1B lineage, is also homozygous lethal. It may be that detrimental effects of ESIA and T797I (and subsequently I797V) observed on the *D. melanogaster* protein are ameliorated by other substitutions in the ATPα1 sequence background of fireflies. However, even if active and resistant, ATPα1B has the lowest expression among the four paralogs (**Figure 2C**), implying that it may contribute little to overall CTS resistance in *Photuris*.

A more dramatic series of substitutions implicated in CTS resistance occurs along the lineage leading to *Photuris* ATPα1 paralogs C and D (**Figure 2B**). We engineered most of these CTS-relevant substitutions (Y108F+Q111E+A112S+V115L+E117T+A119N+D120N, hereafter "FESLTNN") into the *D. melanogaster* ATPα1 protein. The FESLTNN combination results in an additional 3-fold increase in NKA CTS-resistance over ES alone **(Figure 3B; Table S4)**. FESLTNN adults also exhibit exceptionally high rates of survival upon CTS exposure (**Figure 3C)**. Further dissection of individual substitution effects reveals that A119N and the combination

(Q111E+A112S+A119N, hereafter "ESN") confer substantial CTS resistance to NKA (almost 3-fold and 16-fold, respectively). The level of NKA CTS resistance for ESN (16-fold) is only slightly lower than for FESLTNN (18-fold, **Table S4**), implying that the marginal effect of A119N is nearly sufficient to explain the difference between ES and FESLTNN. A119N alone also appears to be sufficient to confer levels of adult resistance to CTS exposure that are comparable to ES, ESN and FESLTNN (**Supplementary Figure S5C**).

Evaluation of the trade-offs associated with resistance conferred by various evolutionary intermediates offers further insight into the likely evolutionary paths used to evolve CTS resistance along the C/D paralog lineage (**Figure 3D**; **Supplementary Figure S5**). Notably, "ES", which represents ancestral states in this lineage, confers substantial CTS-resistance, but at the cost of neurological defects (**Figure 3D**). While adding A119N to the ES background (i.e., ESN) results in even higher CTS resistance, this comes at the cost of even greater neurological dysfunction. Interestingly, we find that ESN in combination with other substitutions added to the C/D paralog lineage (i.e. FESLTNN) results in a similar level of CTS resistance, but with substantially reduced neurological dysfunction. Taken together, our results reveal that serial rounds of gene duplication and neofunctionalization led to stepwise increases in the level of CTS resistance in *Photuris* over time with substitutions A119I, Q111E+A112S and I119N being key evolutionary steps. In addition, substitutions at other sites implicated in CTS resistance, while not contributing much to resistance itself, nonetheless appear to play a critical role in ameliorating pleiotropic costs associated with key resistance substitutions.

The evolution of CTS resistance in prey firefly species.

The *Photinus* NKA protein is also highly resistant to CTS inhibition *in vitro* (**Figure 1B**). However, in contrast to the dramatic patterns of neofunctionalization in *Photuris*, the sole copy of ATPα1 in *Photinus* curiously lacks substitutions at known CTS-insensitivity sites other than V119I (**Figure 2**; **Supplementary Figure S1**), which has a significant but relatively small effect (**Figure 2B, Table S4**). Notably absent in prey firefly species are substitutions at sites 111 and 122 which are most often associated with large effects on CTS resistance in species with a single copy of ATPα1 (Zhen et al. 2012; Yang et al. 2019).

In order to search for previously undocumented CTS-resistance sites throughout the protein, we queried all substitutions, naive to previously known functional importance, in a large alignment of ATPα1 sequences from CTS-adapted and non-adapted insects (see Methods). Of potential candidate substitutions in the *Photinus* lineage, only one (I787M) exhibits a strong signature of parallel evolution in multiple CTS-adapted taxa, including CTS-producing fireflies and *Photuris* (**Figure 4A**). Using CRISPR-Cas9 engineering of *D. melanogaster*, we show that I787M has a significant effect on CTS resistance of the enzyme *in vitro* (a 3-fold increase; **Figure 4B, Table S4**). Despite its relatively modest effect on CTS-resistance of the enzyme *in vitro*, I787M has a substantial effect on the tolerance of adult *D. melanogaster* to CTS exposure (**Figure 4C**) and is not associated with substantial neurological dysfunction (**Figure 4D**). Thus, I787M is a previously unreported determinant of CTS-resistance that shows a high degree of parallelism among CTS-adapted insects.

Discussion

CTS resistance and the use of CTS for defense have convergently evolved in a large number of species. Our study reveals that the first steps toward CTS resistance evolution in fireflies (A119V, V119I) were likely taken before predatory specialization on fireflies as a source of CTS emerged in *Photuris*. One possible explanation for these shared steps is that *de novo* production of CTS is ancestral to fireflies and that the ability to do this was subsequently lost in *Photuris* as they opted for predation as an alternative source of these toxins. However, there is little evidence for this based on the phylogenetic distribution of CTS production in fireflies (**Figure 4A** and see (Berger et al. 2021)). An alternative hypothesis is that these steps may reflect exaptations in fireflies unrelated to CTS metabolism. This is supported by the widespread distribution of substitutions at site 119 among insect taxa that are not adapted to CTS (Taverner et al. 2019). Interestingly, A119N – a key substitution underlying resistance of neofunctionalized *Photuris* paralogs – is present in all Hymenopteran species surveyed to date (Taverner et al. 2019). As most Hymenopterans are not associated with CTS, A119N may function as an exaptation that facilitated herbivorous wasp specialization on CTS containing hostplants (Dobler et al. 2015)

and parasitoid wasp species predation on CTS-adapted herbivorous insects (Groen and Whiteman 2021).

Despite initial shared steps toward CTS resistance taken early in firefly diversification, our study also highlights the distinct dynamics of CTS resistance evolution associated with their different ecological roles. Although both *Photuris* and other fireflies are protected by the same class of CTS toxins, they nonetheless face different biochemical and physiological challenges posed by *de novo* production (most firefly genera) versus sequestration from a food source (*Photuris*) (Heckel 2014; Petschenka and Agrawal 2016; González et al. 1999). Notably, the dramatic repeated duplication and neofunctionalization of ATPα1 in *Photuris* resembles the strategy employed by several CTS-adapted herbivores that sequester CTS from a food-source (Dobler et al. 2012; Petschenka et al. 2017; Yang et al. 2019; Zhen et al. 2012; Dobler et al. 2019, 2015). We speculate that the duplication and neofunctionalization of ATPα1 in *Photuris* may have been driven by the evolution of firefly predation in the *Photuris* lineage, which imposed similar biochemical and physiological challenges to those experienced by herbivores that sequester CTS from hostplants.

We have shown that intermediate stages in the evolution of resistant forms of NKA in *Photuris* are associated with substantial enzymatic and physiological dysfunction when engineered into *D. melanogaster*. This dysfunction would likely represent a substantial negatively pleiotropic barrier to the evolution of CTS resistance if the ATPα1 gene existed as a single copy in *Photuris*. We propose that these negative pleiotropic effects were largely avoided by duplication and neofunctionalization in the *Photuris* lineage, allowing this lineage to specialize on consuming and sequestering toxins from CTS-containing prey. Thus, our work implicates duplication and neofunctionalization as a key factor in the diversification of species roles within an ecological community.

There remain some interesting and puzzling differences between insect herbivores and fireflies with respect to the molecular basis of CTS-resistance via substitutions to ATPα1. A recent study showed that three amino acid substitutions are sufficient to account for the entire difference in NKA CTS-resistance observed between the wild-type proteins of *D. melanogaster* and the

monarch butterfly, *Danaus plexippus* (Karageorgi et al. 2019). In contrast, our attempts to engineer known CTS-resistance substitutions of fireflies into *D. melanogaster* NKA fall short of the level of CTS-resistance level of wild-type firefly proteins (**Supplementary Figure S7**). This suggests wild-type firefly NKAs achieve high levels of CTS-resistance via substitutions at other sites in ATPα1. Previous attempts to map determinants of CTS resistance using saturation mutagenesis are likely to have missed sites with relatively small effects on CTS resistance (Croyle et al. 1997). This may explain why the I787M, discovered here using phylogenetic methods, was missed in previous screens for CTS-resistance mutations. The gap between engineered-*Drosophila* and wild-type firefly NKA CTS-resistance, and the lack of obvious candidate substitutions in *Photinus*, suggests that there are likely to be other, as yet undiscovered, determinants of CTS resistance in firefly NKAs.

Acknowledgements

We thank the Fireflyers International Network for providing samples of *P. frontalis* (notably H. Morgan and P. Shaw) and their valuable natural history input. We thank P. Reilly for advice on CRISPR-cas9 design, A. Taverner for help with fly crosses, and C. Han for advice on variant calling analysis. We thank S. Stiehler and M. Jang for technical assistance. Finally, we thank AM for inspiration. This work was funded by the National Institutes of Health R01 GM115523 to PA, AG059385 to MJP, and DFG PE2059/3-1 and the LOEWE program of the State of Hesse (Insect Biotechnology & Bioresources), Germany to GP.

Author contributions

LY and PA designed the study; LY, FB, MA, RV, MW and PA collected and prepared firefly samples; LY, FB, YZ, MA and JP generated sequence data; LY, FB and PA performed data analysis; MJP, BPR and ADT generated phiC31/cre-lox engineered flies. LY generated a subset of CRISPR/cas9 engineered flies; LY, FB and GP performed functional assays; LY and PA wrote the paper with input from the other authors.

Figure Legends

Figure 1. Na^+,K^+-ATPase (NKA) resistance to cardiotonic steroids (CTS) in predatory and prey firefly species. (A) Female *Photuris versicolor* preying on a *Photinus pyralis* male (photo by Lu Yang 2017). (B) CTS-inhibition assay on firefly nervous system NKA shows that both Photuris versicolor (red) and *Photinus pyralis* (blue) are resistant to ouabain (a representative CTS). Mean relative ATPase activity of NKA (closed circles) is plotted as a function of increasing molar (M) concentrations of the CTS ouabain. Open circles indicate biological replicates (n=3 for *Photuris* and n=2 for *Photinus*). The NKA of both fireflies are significantly more resistant than that of the fruit fly, *D. melanogaster* (**Table S4**). The fitted curves for *Photinus pyralis* and *Photuris versicolor* assume monophasic and biphasic inhibition functions, respectively (see Methods).

Figure 2. Molecular evolution of ATPα1 in fireflies. (A) A maximum likelihood genealogical tree based on ATPα1 protein-coding sequences (Methods and **Supplementary Figure S1** for more detail). ATPα1 of CTS-producing firefly species are shaded in blue and four *Photuris* ATPα1 paralogs A-D are indicated in increasingly darker shades of red. White circles indicate three sequential rounds of duplication in the *Photuris* lineage. Substitution patterns are shown only for sites with known roles in CTS-resistance, except for site 787, which is newly discovered in this study. The reference sequence corresponds to the reconstructed ancestral sequence for beetles. Dots indicate identity with the ancestral state and letters represent derived amino acid substitutions. The phylogenetic position of *Bicellonychia wickershamorum*, which is not associated with CTS, has 93% bootstrap support and is consistent with phylogenetic reconstructions based on multiple loci (Chen et al. 2019; Höhna et al. 2022). **(B)** Schematic graph showing key amino acid substitutions associated with CTS-resistance inferred to have occurred in species and paralog lineages. See **Figure S1** for more details. **(C)** Tissue-specific expression of ATPα1 paralogs in *Photuris versicolor* females (see also **Table S2, Supplementary Figures S2 and S3**). Column width corresponds to relative proportion of total normalized ATPα1 expression summed across paralogs in *Photuris*, and shaded segments to relative levels of expression of the four ATPα1 paralogs in each tissue.

Figure 3. Functional effects of *Photuris* paralog-specific substitutions. (A) Engineered fly lines generated in this study. Only sites implicated in CTS-resistance are shown. States for the CTS-sensitive *D. melanogaster* strain (w^{1118}) used to generate engineered lines are denoted "WT" for "wild-type". Each of the next three lines in increasingly darker shades of red carries a subset of substitutions specific to ATPα1 paralogs A-C. Results for a number of other engineered lines can be found in **Supplementary Figures S4-S6**. (B) CTS-inhibition assays for NKA isolated from heads of WT and engineered fly lines. Mean relative activities (filled circles) are plotted as a function of increasing concentrations of the CTS ouabain. Each mean is the average of three biological replicates (see **Methods**). Solid lines represent the least squares fit model (see Methods) as in **Figure 1**. (C) CTS-tolerance of wild-type and engineered adult flies. Survival of adult flies upon seven days exposure to increasing concentrations of CTS (0, 5, 10, 15, 20 mM ouabain). Points represent the average of three biological replicates (n=20 individuals each), and whiskers correspond to standard errors. (D) Levels of neural dysfunction and enzyme resistance to the CTS ouabain for wild-type (WT) and engineered fly lines. The neural dysfunction assay (y-axis) measures the recovery time following seizures induced by mechanical overstimulation (aka "bang sensitivity" assay) of 14-day old male flies (times are capped at 120 seconds). 28-43 individuals (open circles) are assayed for each line, and the mean and 95% bootstrap confidence bounds are indicated as points and whiskers, respectively. The level of enzyme resistance to CTS (x-axis) is measured as IC50 in an ouabain-inhibition assay (see **Methods**). Plotted is the mean IC50 of three biological replicates (each the average of three technical replicates) and a 95% confidence interval for the estimate.

Figure 4. Evolutionary and functional analysis reveals a new CTS-resistance substitution, I787M. (A) Recurrent appearance of I787M in CTS-associated herbivores (green lineages), CTS-producing prey fireflies (blue lineages) and predatory *Photuris* fireflies (red lineage). See **Supplementary Figure S6** for more details. (B) Estimates of the $\log_{10}(IC_{50})$ of NKA of wild-type and engineered fly lines in CTS-inhibition assays. The $\log_{10}(IC_{50})$ of I787M flies (-6.37, 95% CI: -6.39, -6.36) is 2.9-fold higher than that of WT (w^{1118}) control flies (-6.83, 95% CI: -6.87, -6.80). Each estimate is based on three biological replicates (each with three technical replicates). (C) CTS-tolerance of adult wild-type and engineered flies. Engineered flies carrying I787M exhibit higher survival rates upon seven-day CTS exposure. (D) Neural dysfunction as measured by the "bang sensitivity" assay. The assay measures the time to recovery from seizures induced by mechanical over-stimulation (as in **Figure 3**). Open circles correspond to individual flies. Filled circles to the right are means with 95% CI whiskers. I787M individuals are somewhat more susceptible to mechanical over-stimulation than WT (Wilcoxon test p= 3.4e-5), but the impairment is less severe than observed for some other engineered strains. See **Figure 3** for genotypes of A119I, ES, FESLTNN.

STAR Methods

Resource Availability

Lead Contact

Further information and requests on methods can be directed to Dr. Peter Andolfatto pa2543@columbia.edu

Materials Availability

Plasmids used in this study are available upon request. This study did not generate new unique reagents.

Data and Code Availability

Data generated during this study are available through links provided in the Key Resources Table. Nucleotide sequences (CDS) of ATPα1 have been submitted to GenBank (Accession Numbers: MT897473-MT897482). RNA-seq data for *Photinus pyralis* and *Photuris versicolor* have been deposited in the Sequence Read Archive (BioProject PRJNA891248 and PRJNA891306, respectively).

Experimental Model and Subject Details

Method Details

Firefly collection and data sources

Photuris versicolor and *Photinus pyralis* were collected in Princeton, NJ, USA during the summer months of 2017, 2018 and 2022. Samples were immediately stored in -80ºC with or without RNAlater (InvitrogenTM) depending on the planned downstream experiments. For other species, we used publicly available data (see **Table S1**).

RNA-seq data generation and ATPα1 reconstruction

Total RNA from muscle (thoracic or leg), heads and gut of male *Photinus*, female and male *Photuris* fireflies was extracted with TRIzol (Ambion, Life Technologies) following the

manufacturer's protocol. For male *Photinus* and female *Photuris* samples, RNA-seq libraries were prepared with TruSeq RNA Library Prep Kit v2 (Illumina) and sequenced on Hiseq4000 (Genewiz, South Plainfield, NJ, USA). Reads were trimmed for quality and length using TQSfastq.py (https://github.com/JaneliaSciComp/msg/blob/master/TQSfastq.py) with default parameters. For male *Photuris* samples, RNA-seq libraries were prepared with TruSeq RNA Library Prep Kit v3 (Illumina) and sequenced on HiSeq X (PSOMAGEN, Inc.). Reads were trimmed for adapters but not for quality using trim_galore (v0.6.7) with cutadapt (v1.18). The three RNA-seq datasets were used to generate *de novo* transcriptome assemblies using Trinity v2.2.0 [Haas, 2013] with default parameters. Beetle ATPα1 sequences (Zhen et al., 2012) were used as initial queries to BLAST against firefly transcriptome assemblies. Reconstructed ATPα1 sequences for *Photinus pyralis* and *Photuris versicolor* were then used as templates to identify ATPα1 sequences in *de novo* transcriptome assemblies from other firefly species. Since *de novo* assembly of *P. versicolor* revealed four distinct paralogs of ATPα1, we set out to determine the ages of duplication events but surveying closely related species *Photuris frontalis* and *Bicellonycha wickershamorum* (**Table S1**). For both species, we used *de novo* assembly of previously published RNA-seq (as above) and mapping of RNA-seq reads to *P. versicolor* sequences for paralogs A-D. Nearly identical paralogs were detected in *P. frontalis* but only one copy of ATPα1 was detected in *B. wickershamorum.*

Confirmation of ATPα1 duplicates in *P. versiciolor*

The four reconstructed ATPα1 paralogs (A-D) of *Photuris versicolor* were confirmed by PCR-cloning and sequencing using the following primers: Ptu_ver_AF: CGCTGACTTTGATTCATCCCCAGT, Ptu_ver_AR: TTGGCAGTGCGCATCATTCT, Ptu_ver_BF: TCGGAGTTTGGCCGTACAGA, Ptu_ver_BR: TTGGTCAGTGAACGGCAGTG, Ptu_ver_CF: TCGACTTCAGGATTTGTTGACGG, Ptu_ver_CR: TGGCAGTACGCACCATTCAC, Ptu_ver_DF: CGTTCAGACTCATACCGTGTAGC, Ptu_ver_DR: TGAACTCATCCGTAACCATGCAG. ATPα1 paralogs were amplified from cDNA using Phusion High-Fidelity DNA Polymerase (Thermo Fisher Scientific) and separated by agarose gel electrophoresis. The appropriate bands were gel-extracted and cleaned with QIAquick PCR Purification Kit (Qiagen). Purified PCR products were 3′A-tailed using Taq polymerase (NEB) and cloned into TOPO TA-cloning vector (Invitrogen). Plasmids with inserts

were identified and isolated using colony-PCR. Tn5-tagmentation libraries (Picelli et al. 2014) were prepared for each plasmid and indexed using customized Illumina-style i7 and i5 PCR primers added with 10 cycles of PCR. The libraries were pooled and sequenced with 150 nt, paired-end reads on a Illumina MiSeq Nano flowcell. 10,000 pair-end reads per plasmid were randomly sampled, trimmed for quality and *de novo* assembled using Velvet (Zerbino & Birney, 2008) and Oases (Schulz, Zerbino, Vingron & Birney, 2012). The sequences for each paralog were aligned and visualized in SeaView (Gouy, Guindon, & Gascuel, 2009).

Phylogeny estimation and reconstruction of ancestral states

Firefly ATPα1 protein-coding sequences (as described above) together with previous ATPα1 sequences of four outgroup species *Agrilus planipennis*, *Megacyllene robiniae*, *Cyrtepistomus castaneus* and *Plagiodera versicolora* (**Table S1**) were aligned using MUSCLE (v 3.8.425). The first 47 amino acids and the 3'end of *Megacyllene robiniae*, *Cyrtepistomus castaneus* and *Plagiodera versicolora* were trimmed to produce an alignment with no gaps or missing data. A phylogenetic tree for ATPα1 sequences was estimated using maximum likelihood with PhyML (v 3.3.20180621) with the GTR model and default parameters. Ancestral sequences and substitutions along specific-lineages were estimated from predicted protein sequences using PAML's codeml function (v 4.9) with the following parameters: model=1, NSites=0, kappa=1.6, RateAncestor=2 (Yang, 1997).

To look for substitutions that occur recurrently in CTS-associated species, we combined the multispecies alignment of Taverner et al. (2019), which includes 174 predicted ATPα1 sequences from 161 insect species, with our alignment for firefly species (above). Considering all amino acid substitutions, naive to functional importance, we looked for those that 1) are present in at least 3 out of 7 *Photinus* species, 2) are not shared with direct outgroups, e.g., *Pyractomena*, 3) are common in other CTS-associated species relative to other species. One site, and one substitution in particular (I787M) passes these filter criteria. I787M has independently evolved in five insect orders, and 6 out of 7 times it occurred in insects that either sequester or produce CTS (**Supplementary Figure S6**).

Differential expression analysis

Photuris versicolor females were fed with *Photinus pyralis* one day before dissection. RNA-seq data was generated as described in earlier sections. Newly reconstructed ATPα1 sequences were blasted against our male *Photuris de novo* transcriptome with default parameters (BLAST 2.13.0+) and all the hits were removed to be replaced by our own annotated copies. Reads were mapped on this modified transcriptome using bwa mem (v 0.7.17) (Li 2013) and processed using SAMtools (v 1.15.1) (Li et al. 2009). Counts were done by htseq-count (v 2.0.2, parameters: -a 0 --nonunique all). In order to use htseq-count, a gff3 file was made for our transcriptome with the perl script gmod_fasta2gff3.pl (https://github.com/GMOD/Chado/). We used inverted beta-binomial (ibb) tests (Pham & Jimenez, 2012) to determine the significance of difference of expression level among tissues and paralogs, and a standard Bonferroni correction was applied to account for multiple tests (**Table S2**). To visualize the differential expression among species, tissues, and paralogs, counts were normalized using the counts function (normalized=TRUE) of the R package DeSeq2 (Love et al. 2014). Mekko chart was plotted using ggplot2 and mekko package implemented in R.

CRISPR-cas9 engineered fly lines.

A119I:

CRISPR-mediated mutagenesis of *D. melanogaster* was performed by WellGenetics Inc. using modified methods of Kondo and Ueda (2013): gRNA was designed and cloned into an expression vector containing a U6 promoter (pBFv-U6.2) and Cas-9 protein is supplied by a germline expression vector (pBFv-nosP-Cas9). ~1 kilobase homology arms were amplified using Phusion High-Fidelity DNA Polymerase (Thermo Scientific) from genomic DNA of the injection strain w^{1118}. A plasmid donor template for repair, pUC57-Kan-A119I-PBacDsRed, was constructed containing 3xP3-DsRed and two homology arms flanked by PBac terminals ("TTAA"). The substitution A119I (standardized amino acid residue numbering) was introduced into ATPα coding sequence via point mutations changing the codon "GCC" to "ATC". Additional synonymous substitutions were added to eliminate three targeted PAM sites. For sequences of gRNA and homology arms see (**Table S3**). gRNA and donor plasmid constructs were confirmed by sequencing prior to injection. *ATPα*-targeting gRNAs and donor plasmid

were microinjected into embryos 210 embryos of the strain *w*^{1118}*; attP40{nos-Cas9} / CyO*. Of 11 surviving G0 adults, 10 crosses to strain *w[*];;TM6B, Tb[1] / TM2, y+* were fertile and one was confirmed DsRed+. Insertion of the construct into the correct location was confirmed both PCR and sequencing. *PBac-DsRed* was subsequently excised by first crossing to the strain *w[*]; CyO, P{Tub-PBac}/ Sp; +/TM6B* (Bloomington #8285) and subsequently to *w[*]; TM3, Sb[1] Ser[1]/TM6B, Tb[1]* (Bloomington #2537). Repeated rounds of sib-mating were used to obtain stable homozygous lines. Precise excision of *PBacDsRed* and correctly-edited genome sequence was validated by genomic PCR and sequencing.

Y108F-Q111E-A112S-S115L-E117T-A119N-D120N ("FESLTNN"):

Engineered line Y108F-Q111E-A112S-S115L-E117T-A119N-D120N was generated by WellGenetics Inc. (Taipei, Taiwan) using the same methods as described for A119I (including the same homology arms and gRNA). 222 *w*^{1118}*; attP40{nos-Cas9}/CyO* embryos were injected with the *ATP*α-targeting gRNAs and donor plasmid. Of 18 surviving G0 adults, 15 were fertile in crosses to strain *w[*];;TM6B, Tb[1] / TM2, y+* and two were DsRed+. Both DsRed+ lines were PCR-sequence confirmed to contain correct insertions and processed to excise *PBac-DsRed* (as above). Each line was repeatedly sib-mated to generate homozygous lines and genome sequences were validated by genomic PCR and sequencing.

Q111E-A112S-A119I-D120A ("ESIA"):

Engineered line Q111E-A112S-A119I-D120A was generated by WellGenetics Inc. (Taipei, Taiwan) using the same methods as above (including homology arms and gRNA). Out of 645 microinjections of *ATP*α-targeting gRNAs, a donor plasmid and a plasmid carrying *hsp70Bb-cas9* into *w*^{1118}, three lines were DsRed+ and validated carrying the correct insertion. However, after *PBac-DsRed* excision and repeated sib-mating, no homozygous mutant flies could be obtained.

T797I:

Engineered line T797I was generated by WellGenetics Inc. (Taipei, Taiwan) using a unique gRNA and ~1kb homology arms (see Table S3). An additional mutation of a BsaI site GGTCTC → CGTCTC in the upstream homology arm in the donor plasmid was introduced to facilitate

Golden Gate cloning. Of 422 injections of *ATPα*-targeting gRNAs, a donor plasmid *hsp70Bb-cas9* into w^{1118}, two lines were DsRed+ and validated as carrying the correct insertion. However, after *PBac-DsRed* excision and repeated sib-mating, no homozygous mutant flies could be obtained for either line.

F786Y and I787M:

Engineered lines F786Y and I787M were generated in-house with CRISPR-cas9 homology-dependent repair (HDR) using one gRNA and a template single-stranded donor oligonucleotide (ssODN). The designed gRNA (5'-TGGTATATCGCAGAGGATGA[AGG]-3') showed no off-target sites by *in silico* prediction (using a web-based tool called "desktop", which is now deprecated). Oligonucleotides (IDT) were annealed to generate a T7-gRNA expression template (**Table S3**). This template was PCR amplified, size verified on a 2% agarose gel, purified using a QIAquick spin column (Qiagen), and eluted in 30 µl Elution Buffer (Qiagen). *In vitro* transcription of gRNA templates was carried out by MEGAscript T7 Transcription Kit following the manufacturer's protocol (Fisher Scientific). DNA and proteins were removed with turbo DNAse and phenol:chloroform:isoamyl alcohol, respectively. RNA was purified with equal volume of isopropanol, washed twice with 70% ethanol, resuspended in 30 µl RNAse-free water, and quality checked on a Bioanalyzer (Agilent). Asymmetrical ssODN design was implemented to achieve better performance (Richardson et al. 2016). Synonymous mutations were introduced to facilitate downstream PCR screening (**Table S3**). ssODNs were synthesized through IDT (Coralville, Iowa, USA)'s Ultramer DNA Oligo service. 20 µl mixture of 100 ng/µl gRNA and 500 ng/µl ssODNs and Cas-9 mRNA were injected into 200 embryos of the line w^{1118}*; attP40{nos-Cas9} / CyO* by Rainbow Transgenic Flies, Inc (Camarillo, CA, USA). Approximately 5% of G0 offspring were fertile and were crossed to *w[*]; TM3, Sb[1] Ser[1]/TM6B, Tb[1]* (Bloomington #2537). G1 flies were separated into individual vials and again crossed to the same double balancer line (Bloomington #2537). After 3-5 days, when enough eggs were laid, the genomic DNA of G1 flies was extracted using SquishPrep protocol. A 289-bp region spanning sites 786 and 787 was PCR-amplified with primers compatible with adding customized Illumina-style i5 and i7 indexes (Yang et al. 2019) (**Table S3**), and paired-end 150 nt sequenced on Illumina MiSeq Nano (Genomics Core Facility, Princeton, NJ, USA). Three independent lines of F786Y and two lines of I787M were obtained and confirmed by

sequencing. Progeny of G1 flies with the substitution F786Y or I787M were selected and sib-mated to obtain homozygous lines.

Additional lines engineered using the method of Taverner et al. (2019).

Lines carrying Q111E, A112S, and/or A119N were generated using the same method described in ref. (Taverner et al. 2019). Substitutions, either individually or in combination, were engineered into the vector *pGX-attB-ATPα2-6b* using Quick-change Lightening site-directed mutagenesis kit (Agilent). These plasmid constructs were injected into a white-eyed founder line w^{1118}*;;ATPαΔ2-6b attP/TM6B,Tb1* by Rainbow Transgenic Flies, Inc (Camarillo, CA, USA) following their standard protocol. Lines with successfully integrated constructs (i.e. indicated by red/pink eyes) were reduced with cre-loxP excision by crossing to y^1, w^{67c23}, *P{y[+mDint2]=Crey}1b;; D*/TM3,* Sb^1 (Bloomington #851) and succesfully reduced lines were balanced by crossing to *w*;;*ry^{506} Dr^1*/TM6B, P{w[+mC]=Dfd-EYFP}3,* Sb^1*,*Tb^1*,*ca^1 (Bloomington 8704). Fluorescent offspring were sib-mated, and non-fluorescent Tb^+*,*Sb^+ larvae were selected to generate stable homozygous lines. Substitutions were validated by PCR and sequencing.

CTS tolerance assay

Fireflies are protected by lucibufagins, a class of cardiotonic steroids ("CTS"). To measure the tolerance of engineered fly lines to CTS exposure, we introduced adult flies to food media containing varying concentrations of the representative CTS ouabain (ouabain octahydrate, Sigma-Aldrich, Cat# O-3125) and recorded how many of adults survived after 7 days. We used 0.7 grams of dried instant media (Flystuff (66-117) Nutri-fly Instant) reconstituted in a standard fly vial with 3.5 ml of 0, 5, 10, 15, or 20 mM ouabain solutions. Although the physiologically relevant concentrations of lucibufagins in fireflies are unknown, a previous study showed that wild-type flies exhibited high fatality rates upon exposure to 5 mM ouabain (Taverner et al. 2019). Reconstituted food was allowed to set for 30 minutes, and a small piece of Kimwipe tissue was added to absorb the moisture. 10 male and 10 female flies that had enclosed within 7 days were placed in each vial (three replicates per line and concentration), and kept at 25ºC, 50% humidity for 7 days. Mortality rate was measured by counting the number of living flies after 7 days. Mortality was not sex-dependent, as expected based on a previous study (Taverner et al.

2019). The Cochran-Mantel-Haenzel test implemented in R was used to assess significant differences between ouabain treatments (5/10/15/20 mM) versus no ouabain.

Enzyme inhibition assays

CTS inhibit the ATPase activity of NKA. The principle of enzyme inhibition assays is to determine the ATPase activity of NKA by photometrically measuring the phosphate released from ATP during enzymatic hydrolysis at various concentrations of CTS. These assays were performed on both wild-caught fireflies and on engineered fly lines. All samples were stored in -80ºC to minimize protein degradation. For fireflies, the nervous tissue was freshly dissected as input material, and 7-15 fireflies together made one biological replicate. For flies, 90 heads were shacked off from frozen flies and pooled together for one assay. Samples were prepared and the activities of NKA were measured following the procedures described in references (Petschenka et al. 2017, 2013). Tissues were suspended and homogenized in deionized water using a glass grinder (Wheaton) on ice. Homogenates were freeze-dried (Christ, Alpha 2-4 LDPlus) overnight, and lyophilisates were reconstituted and split into three technical replicates. Samples were incubated in 6 (firefly) or 12 (fly) increasing concentrations of ouabain solutions (100 mM NaCl, 20 mM KCl, 4 mM $MgCl_2$, 50 mM imidazol, and 2.5 mM ATP) at 37 ºC for 20 minutes. A non-inhibited positive control was carried out without the addition of ouabain, and the negative control was deprived of both ouabain and KCI (inactive NKA) to correct for a background value. Absorbance was measured at 700 nm on a CLARIOstar microplate reader (BMG Labtech, Germany). Each biological replicate was averaged over three technical replicates, and three biological replicates were assayed for each line or species (with an exception of *Photinus pyralis* that only had two biological replicates).

Relative activities of NKA were estimated for each ouabain concentration as (abs[full activity]-abs[inhibited activity])/(abs[full activity]-abs[background activity])). Curve fitting was performed with the nlsLM function from the minipack.lm library in R using the function

$$\text{Relative Activity} = \frac{1}{(1+10^{-IC50+x})*hs}$$

where, x is the ouabain concentration, $IC50$ is the ouabain concentration corresponding to 50% relative activity, and hs is the slope coefficient. Approximate 95% confidence intervals for IC50 were estimated by parametric bootstrapping as described in ref (Taverner et al. 2019) (**Table S4**).

For *Photuris versicolor*, the inhibition curve does not appear to be monophasic since relative enzyme activity is still ~40% at the highest ouabain concentration. We thus made some simplifying assumptions to estimate approximate IC50s. First, it was assumed that the curve is biphasic, reflecting activities of primarily two enzyme isoforms. This can be justified by the fact that in nervous tissue (from which enzyme preps were made), paralogs ATPα1A and ATPα1C are roughly equally expressed and together account for ~90% of total ATPα expression (**Figure 2C**). We thus used the equation

$$\text{Relative Activity} = \frac{(1-f)}{(1+10^{-IC50_1+x})} + \frac{f}{(1+10^{-IC50_2+x})}$$

where, x is the ouabain concentration, $IC50_1$ and $IC50_2$ are the ouabain concentration corresponding to 50% relative activity for each isoform, respectively, f is the total activity attributable to the second isoform and hs for both enzyme isoforms is assumed to be ~1. Approximate 95% confidence intervals for $IC50_1$ and $IC50_2$ were estimated by parametric bootstrapping as above.

Bang-sensitivity assay

The "bang-sensitivity" assay is a classical test where mutants with defective neurological functions paralyze and experience seizures upon mechanical over-stimulation (Karageorgi et al. 2019; Taverner et al. 2019; Ganetzky and Wu 1982; Palladino et al. 2003). Individual 14-day old male flies were placed in an empty *Drosophila* vial, vortexed at the maximum speed for 20 seconds, and immediately dumped to a surface. The time required for each individual to right itself was recorded (times >120 seconds were pooled into one timepoint). 30-50 flies were tested for each genotype. One engineered strain, ESN, was not assayed due to the poor condition of the flies.

Supplementary Figures

Supplementary Figure S1. Maximum likelihood (ML) phylogeny with posterior probabilities on amino acid states. Estimation of the ML phylogeny and ancestral reconstruction were implemented in PAML ((Yang 2007); see Methods). Numbers on nodes indicate the level of bootstrap support for that particular node. A key finding is that the substitution A119V (in bold orange) evolved prior to the diversification of predatory and prey genera whereas V119I and I787M (asterisks) evolved convergently these genera.

Supplementary Figure S2. Tissue-specific expression of ATPα1 paralogs in *Photuris versicolor* females and males. Column width corresponds to relative proportion of total normalized ATPα1 expression for each tissue summed across paralogs. Shaded segments correspond to relative levels of normalized expression of the four ATPα1 paralogs within each tissue.

Supplementary Figure S3. Tissue-specific expression of ATPα1 paralogs in male *Photinus pyralis* (blue) vs *Photuris versicolor* (red) males. Column width corresponds to relative proportion of total normalized ATPα1 expression across tissues (summed across paralogs in *Photuris*). Shaded segments for *Photuris* correspond to relative levels of expression of the four ATPα1 paralogs within each tissue.

Supplementary Figure S4. Evaluation of intermediate steps in ATPα1B evolution in *Photuris*. (A) Engineered fly lines carrying ATPα1B-associated substitutions, individually and in combination. Note that ESIA is homozygous lethal and was not assayed further. (B) CTS-inhibition assays for NKA isolated from heads of "wild type" (WT, line w^{1118}) and engineered fly lines (see panel A). Mean relative activities (filled circles) are plotted as a function of increasing concentrations of the CTS ouabain. Each biological replicate (n=3, not shown) is the average of three technical replicates. Solid lines represent the least squares fit model (see Methods) (C) CTS-tolerance of adult flies. Survival of adult flies upon seven days exposure to different concentrations of CTS (0, 5, 10, 15, 20 mM ouabain). Points represent the average of three biological replicates, and bars correspond to standard errors. (D) Level of neural dysfunction. The assay measures recovery times following seizures induced by mechanical overstimulation (aka the "bang sensitivity" assay) of 14-day old male flies Times are capped at 120 seconds. 28-43 individuals (open circles) are assayed for each line, and the mean and 95% confidence bounds (estimated by re-sampling) are indicated as points and whiskers, respectively.

Supplementary Figure S5. Evaluation of amino acid substitutions contributing to CTS resistance of ATPα1 paralogs C and D in *Photuris*. (A) A collection of engineered fly lines carrying ATPα1B substitutions. The color code follows that in the main text. (B) CTS-inhibition assays for NKA isolated from heads of w^{1118} (WT) and engineered fly lines. Mean relative activities (filled circles) are plotted as a function of increasing concentrations of the CTS ouabain. Each biological replicate (n=3, not shown) is the average of three technical replicates. Solid lines represent the least squares fit model (see Methods) (C) CTS-tolerance of adult flies. Survival of adult flies upon seven days exposure to different concentrations of CTS (0, 5, 10, 15, 20 mM ouabain). Points represent the average of three biological replicates, and bars correspond

to standard errors. ESN was not assayed due to poor condition of the flies. (D) Level of neural dysfunction. The assay measures recovery times following seizures induced by mechanical overstimulation (aka "bang sensitivity" assay) of 14-day old male flies (times capped at 120 seconds). 28-43 individuals (open circles) are assayed for each line, and the mean and 95% confidence bounds (estimated by re-sampling) are indicated as points and whiskers, respectively.

Supplementary Figure S6. Amino acid states at key sites in ATPα1 of CTS-associated insects and representative outgroups. Amino acid numbering follows the standard numbering scheme based on the sheep (*Ovis ares*) ATP1A1 sequence (see Zhen et al. 2012). CTS-associated insects are highlighted in red. The substitution I787M (at highlighted site 787) appears repeatedly in CTS-associated taxa.

Supplementary Figure S7. CTS-inhibition curves suggest as yet unmapped determinants of CTS resistance in firefly Na^+,K^+-ATPases. (A) Engineering three known CTS resistance-associated amino acid substitutions into *D. melanogaster* Na^+,K^+-ATPAse accounts for ~100% of the CTS resistance of the monarch butterfly protein (data from Karageorgi et al. 2019). Plots are as in **Figure 1** of main text. Dmel_QAN = wild type *D. melanogaster* protein; Dmel_VSH = *D. melanogaster* protein + substitutions Q111V, A119S and N122H; monarch = monarch butterfly (*Danaus plexippus*) protein. In contrast, engineering the known major CTS resistance substitutions observed in fireflies into *D. melanogaster* Na,K-ATPase results in only a fraction of the observed CTS resistance of the *Photinus* (left panel) and *Photuris* (right panel) proteins. The latter pattern points to as yet unmapped determinants of CTS resistance of firefly Na,K-ATPases. w1118 = wild-type *D. melanogaster*. The I787M and FESLTNN constructs are described in **Figures 4 and 3**, respectively. "Photinus" and "Photuris" are as in **Figure 1**.

References

Berger A, Petschenka G, Degenkolb T, Geisthardt M, Vilcinskas A. 2021. Insect collections as an untapped source of bioactive compounds—fireflies (Coleoptera: Lampyridae) and cardiotonic steroids as a proof of concept. *Insects* **12**: 689–698.

Blanco G, Mercer RW. 1998. Isozymes of the Na-K-ATPase: heterogeneity in structure, diversity in function. *Am J Physiol* **44**: 633–650.

Branham MA, Wenzel JW. 2003. The origin of photic behavior and the evolution of sexual communication in fireflies (Coleoptera: Lampyridae). *Cladistics* **19**: 1–22.

Chen X, Dong Z, Liu G, He J, Zhao R, Wang W, Peng Y, Li X. 2019. Phylogenetic analysis provides insights into the evolution of Asian fireflies and adult bioluminescence. *Molecular Phylogenetics and Evolution* **140**: 106600.

Croyle ML, Woo AL, Lingrel JB. 1997. Extensive random mutagenesis analysis of the Na+/K+-ATPase a subunit identifies known and previously unidentified amino acid residues that alter ouabain sensitivity Implications for ouabain binding. *Eur J Biochem* **248**: 488–95.

Dobler S, Dalla S, Wagschal V, Agrawal AA. 2012. Community-wide convergent evolution in insect adaptation to toxic cardenolides by substitutions in the Na,K-ATPase. *Proceedings of the National Academy of Sciences of the United States of America* **109**: 13040–13045.

Dobler S, Petschenka G, Wagschal V, Flacht L. 2015. Convergent adaptive evolution - how insects master the challenge of cardiac glycoside-containing host plants. *Entomologia Experimentalis et Applicata* **157**: 30–39.

Dobler S, Wagschal V, Pietsch N, Dahdouli N, Meinzer F, Romey-Glüsing R, Schütte K. 2019. New ways to acquire resistance: Imperfect convergence in insect adaptations to a potent plant toxin. *Proceedings of the Royal Society B: Biological Sciences* **286**.

Eisner T, Goetz MA, Hill DE, Smedley SR, Meinwald J. 1997. Firefly "'femmes fatales'" acquire defensive steroids (lucibufagins) from their firefly prey. *Proceedings of the National Academy of Sciences of the United States of America* **94**: 9723–9728.

Eisner T, Wiemer D, Haynes L, Meinward J. 1978. Lucibufagins: Defensive steroids from the fireflies Photinus ignitus and P. marginellus (Coleoptera: Lampyridae). *Proceedings of National Academy Society* **75**: 905–908.

Fallon TR, Lower SE, Chang C-H, Bessho-Uehara M, Martin GJ, Bewick AJ, Behringer M, Debat HJ, Wong I, Day JC, et al. 2018. Firefly genomes illuminate parallel origins of bioluminescence in beetles. *eLife* **7**: e36495.

Feng J, Lingrel JB. 1994. Analysis of Amino Acid Residues in the H5-H6 Transmembrane and Extracellular Domains of Na,K-ATPase a Subunit Identifies Threonine 797 as a Determinant of Ouabain Sensitivity'* 1' lining. *Biochemistry* **33**: 4218–4224.

Ganetzky B, Wu CF. 1982. Indirect Suppression Involving Behavioral Mutants with Altered Nerve Excitability in DROSOPHILA MELANOGASTER. *Genetics* **100**: 597–614.

González A, Schroeder FC, Attygalle AB, Svatos' A', Meinwald J, Eisner T. 1999. Metabolic transformations of acquired lucibufagins by firefly ' "femmes fatales"'*. *Chemoecology* **9**: 105–112.

Groen SC, Whiteman NK. 2021. Convergent evolution of cardiac-glycoside resistance in predators and parasites of milkweed herbivores. *Current biology : CB* **31**: R1465–R1466.

Gronquist M, Meinwald J, Eisner T, Schroeder FC. 2005. Exploring uncharted terrain in nature's structure space using capillary NMR spectroscopy: 13 Steroids from 50 fireflies. *Journal of the American Chemical Society* **127**: 10810–10811.

Heckel DG. 2014. Insect Detoxification and Sequestration Strategies. In *Annual Plant Reviews* (eds. C. Voelckel and G. Jander), pp. 77–114, John Wiley & Sons, Ltd, Chichester, UK https://onlinelibrary.wiley.com/doi/10.1002/9781118829783.ch3 (Accessed January 9, 2023).

Höhna S, Lower SE, Duchen P, Catalán A. 2022. A Time-calibrated Firefly (Coleoptera: Lampyridae) Phylogeny: Using Genomic Data for Divergence Time Estimation. *bioRXiv*. https://www.biorxiv.org/content/10.1101/2021.11.19.469195v2.

Holzinger F, Wink M. 1996. Mediation of cardiac glycoside insensitivity in the monarch butterfly (Danaus plexippus): Role of an amino acid substitution in the ouabain binding site of Na+,K+-ATPase. *Journal of Chemical Ecology* **22**: 1921–1937.

Karageorgi M, Groen SC, Sumbul F, Pelaez JN, Verster KI, Aguilar JM, Hastings AP, Bernstein SL, Matsunaga T, Astourian M, et al. 2019. Genome editing retraces the evolution of toxin resistance in the monarch butterfly. *Nature* **574**: 409–412.

Laursen M, Gregersen JL, Yatime L, Nissen P, Fedosova NU. 2015. Structures and characterization of digoxin- and bufalin-bound Na+,K+-ATPase compared with the ouabain-bound complex. *Proceedings of the National Academy of Sciences of the United States of America* **112**: 1755–1760.

Lewis SM, Cratsley CK. 2008. Flash signal evolution, mate choice, and predation in fireflies. *Annual Review of Entomology* **53**: 293–321.

Li H. 2013. Aligning sequence reads, clone sequences and assembly contigs with BWA-MEM. http://arxiv.org/abs/1303.3997 (Accessed March 8, 2023).

Li H, Handsaker B, Wysoker A, Fennell T, Ruan J, Homer N, Marth G, Abecasis G, Durbin R, 1000 Genome Project Data Processing Subgroup. 2009. The Sequence Alignment/Map format and SAMtools. *Bioinformatics* **25**: 2078–2079.

Lingrel JB. 2009. The physiological significance of the cardiotonic steroid/ouabain-binding site of the Na,K-ATPase. *Annual Review of Physiology* **72**: 395–412.

Lloyd JE. 1965. Aggressive Mimicry in Photuris: Firefly Femmes Fatales. *Sciences* **149**: 653–654.

Lloyd JE. 1973. Firefly Parasites and Predators. *The Coleopterists Bulletin* **27**: 91–106.

Love MI, Huber W, Anders S. 2014. Moderated estimation of fold change and dispersion for RNA-seq data with DESeq2. *Genome Biol* **15**: 550.

Meinwald J, Wiemer D, Eisner T. 1979. Lucibufagins. 2. Esters of 12-Oxo-2p,5p, 1 1 a-trihydroxybufalin, the Major Defensive Steroids of the Firefly Photinus pyralis (Coleoptera: Lampyridae). *Journal of the American Chemical Society* **9**: 3055–3060.

Mohammadi S, Herrera-Álvarez S, Yang L, Rodríguez-Ordoñez M del P, Zhang K, Storz JF, Dobler S, Crawford AJ, Andolfatto P. 2022. Constraints on the evolution of toxin-resistant Na,K-ATPases have limited dependence on sequence divergence ed. H.S. Malik. *PLOS Genetics* **18**: e1010323.

Mohammadi S, Yang L, Harpak A, Herrera-Álvarez S, del Pilar Rodríguez-Ordoñez M, Peng J, Zhang K, Storz JF, Dobler S, Crawford AJ, et al. 2021. Concerted evolution reveals co-adapted amino acid substitutions in Na+K+-ATPase of frogs that prey on toxic toads. *Current Biology* **31**: 2530-2538.e10.

Moore DJ, Halliday DCT, Rowell DM, Robinson AJ, Keogh JS. 2009. Positive Darwinian selection results in resistance to cardioactive toxins in true toads (Anura: Bufonidae). *Biology Letters* **5**: 513–516.

Oba Y, Konishi K, Yano D, Shibata H, Kato D, Shirai T. 2020. Resurrecting the ancient glow of the fireflies. *Sci Adv* **6**: eabc5705.

Palladino MJ, Bower JE, Kreber R, Ganetzky B. 2003. Neural Dysfunction and Neurodegeneration in *Drosophila* Na^+/K^+ ATPase Alpha Subunit Mutants. *J Neurosci* **23**: 1276–1286.

Petschenka G, Agrawal AA. 2016. How herbivores coopt plant defenses: natural selection, specialization, and sequestration. *Current Opinion in Insect Science* **14**: 17–24.

Petschenka G, Pick C, Wagschal V, Dobler S. 2013. Functional evidence for physiological mechanisms to circumvent neurotoxicity of cardenolides in an adapted and a non-adapted hawk-moth species. *Proceedings of the Royal Society B: Biological Sciences* **280**.

Petschenka G, Wagschal V, Von Tschirnhaus M, Donath A, Dobler S, Koenig FA. 2017. Convergently Evolved Toxic Secondary Metabolites in Plants Drive the Parallel Molecular Evolution of Insect Resistance. *The American Naturalist* **190**. http://dx.doi.org/10.5061/dryad.20191.

Picelli S, Björklund ÅK, Reinius B, Sagasser S, Winberg G, Sandberg R. 2014. Tn5 transposase and tagmentation procedures for massively scaled sequencing projects. *Genome Res* **24**: 2033–2040.

Richardson CD, Ray GJ, DeWitt MA, Curie GL, Corn JE. 2016. Enhancing homology-directed genome editing by catalytically active and inactive CRISPR-Cas9 using asymmetric donor DNA. *Nature Biotechnology* **34**: 339–344.

Smedley SR, Risteen RG, Tonyai KK, Pitino JC, Hu Y, Ahmed ZB, Christofel BT, Gaber M, Howells NR, Mosey CF, et al. 2017. Bufadienolides (lucibufagins) from an ecologically aberrant firefly (Ellychnia corrusca). *Chemoecology* **27**: 141–153.

Souto PM, Campello L, Khattar G, Miras Mermudes JR, Monteiro RF, Lima da Silveira LF. 2019. How to design a predatory firefly? Lessons from the Photurinae (Coleoptera: Lampyridae). *Zoologischer Anzeiger* **278**: 1–13.

Taverner AM, Yang L, Barile ZJ, Lin B, Peng J, Pinharanda AP, Rao AS, Roland BP, Talsma AD, Wei D, et al. 2019. Adaptive substitutions underlying cardiac glycoside insensitivity in insects exhibit epistasis in vivo. *eLife* **8**. https://elifesciences.org/articles/48224.

Tyler J, McKinnon W, Lord G, Hilton P. 2008. A defensive steroidal pyrone in the Glow-worm Lampyris noctiluca L. (Coleoptera: Lampyridae). *Physiological Entomology* 167–170.

Ujvari B, Casewell NR, Sunagar K, Arbuckle K, Wüster W, Lo N, O'Meally D, Beckmann C, King GF, Deplazes E, et al. 2015. Widespread convergence in toxin resistance by predictable molecular evolution. *Proceedings of the National Academy of Sciences of the United States of America* **112**: 11911–11916.

Yang L, Ravikanthachari N, Mariño-Pérez R, Deshmukh R, Wu M, Rosenstein A, Kunte K, Song H, Andolfatto P. 2019. Predictability in the evolution of Orthopteran cardenolide insensitivity. *Philosophical Transactions of the Royal Society B: Biological Sciences* **374**.

Yang Z. 2007. PAML 4: Phylogenetic Analysis by Maximum Likelihood. *Molecular Biology and Evolution* **24**: 1586–1591.

Zhen Y, Aardema ML, Medina EM, Schumer M, Andolfatto P. 2012. Parallel Molecular Evolution in an Herbivore Community. *Science* **337**: 1634–1637.

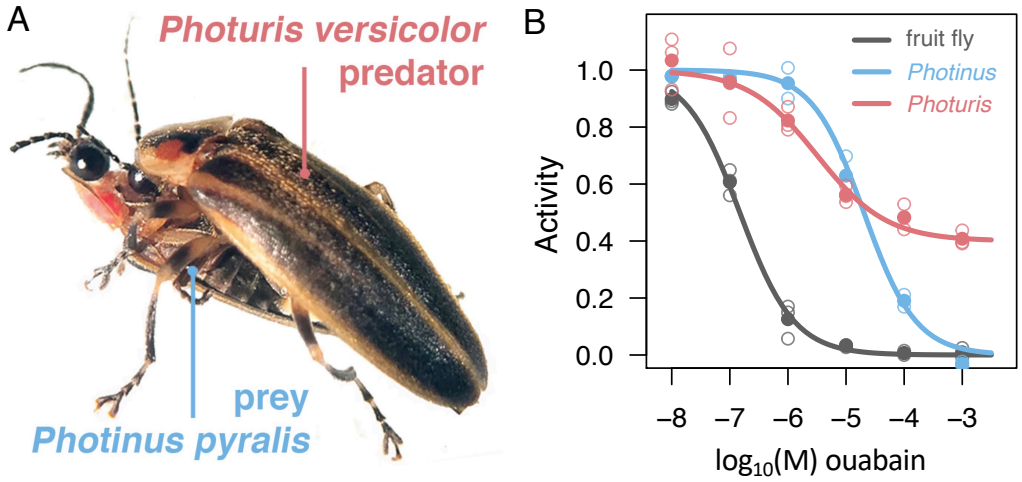

Figure 1. Na^+,K^+-ATPase (NKA) resistance to cardiotonic steroids (CTS) in predatory and prey firefly species. (A) Female *Photuris versicolor* preying on a *Photinus pyralis* male (photo by Lu Yang 2017). (B) CTS-inhibition assay on firefly nervous system NKA shows that both Photuris versicolor (red) and *Photinus pyralis* (blue) are resistant to ouabain (a representative CTS). Mean relative ATPase activity of NKA (closed circles) is plotted as a function of increasing molar (M) concentrations of the CTS ouabain. Open circles indicate biological replicates (n=3 for *Photuris* and n=2 for *Photinus*). The NKA of both fireflies are significantly more resistant than that of the fruit fly, *D. melanogaster* (Table S4). The fitted curves for *Photinus pyralis* and *Photuris versicolor* assume monophasic and biphasic inhibition functions, respectively (see Methods).

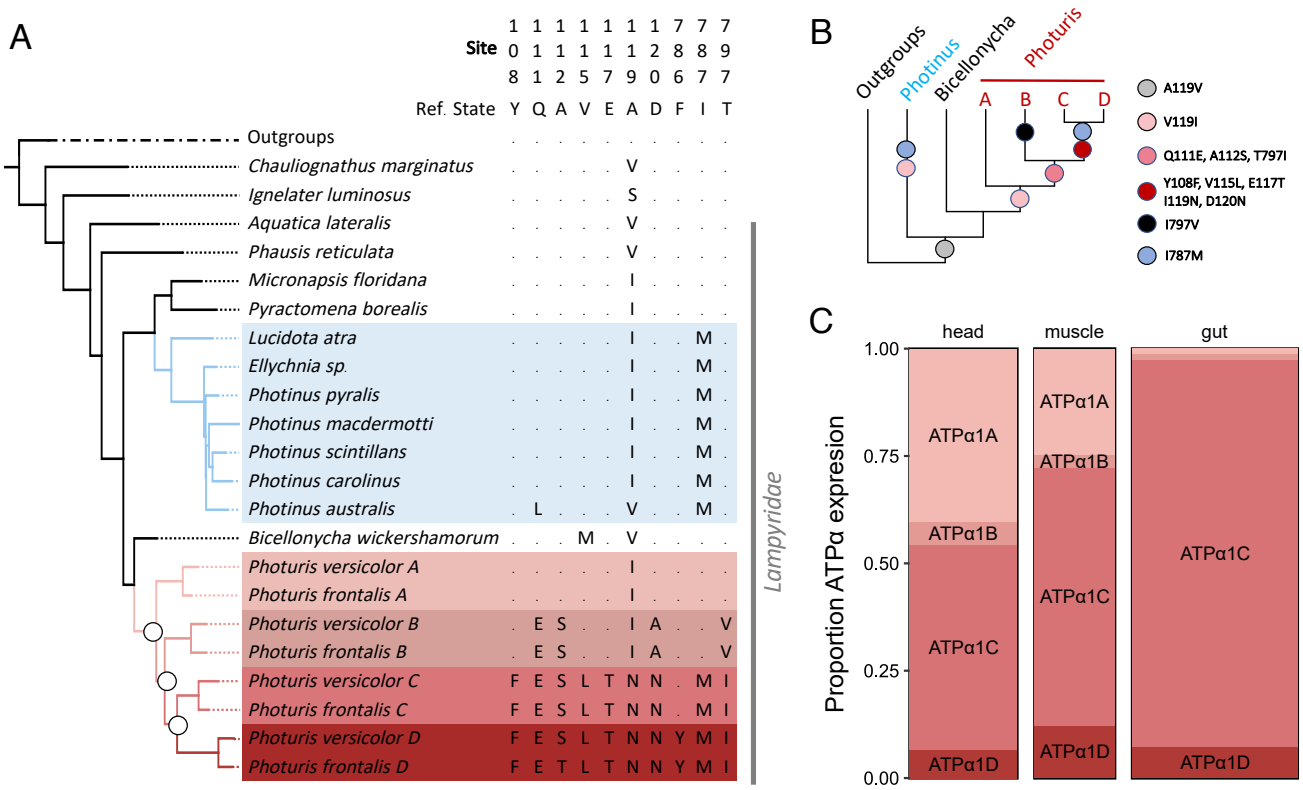

Figure 2. Molecular evolution of ATPα1 in fireflies. (A) A maximum likelihood genealogical tree based on ATPα1 protein-coding sequences (Methods and **Supplementary Figure S1** for more detail). ATPα1 of CTS-producing firefly species are shaded in blue and four *Photuris* ATPα1 paralogs A-D are indicated in increasingly darker shades of red. White circles indicate three sequential rounds of duplication in the *Photuris* lineage. Substitution patterns are shown only for sites with known roles in CTS-resistance, except for site 787, which is newly discovered in this study. The reference sequence corresponds to the reconstructed ancestral sequence for beetles. Dots indicate identity with the ancestral state and letters represent derived amino acid substitutions. The phylogenetic position of *Bicellonychia wickershamorum*, which is not associated with CTS, has 93% bootstrap support and is consistent with phylogenetic reconstructions based on multiple loci (Chen et al. 2019). **(B)** Schematic graph showing key amino acid substitutions associated with CTS-resistance inferred to have occurred in species and paralog lineages. See **Figure S1** for more details. **(C)** Tissue-specific expression of ATPα1 paralogs in *Photuris versicolor* females (see also **Table S2, Supplementary Figures S2 and S3**). Column width corresponds to relative proportion of total normalized ATPα1 expression summed across paralogs in *Photuris*, and shaded segments to relative levels of expression of the four ATPα1 paralogs in each tissue.

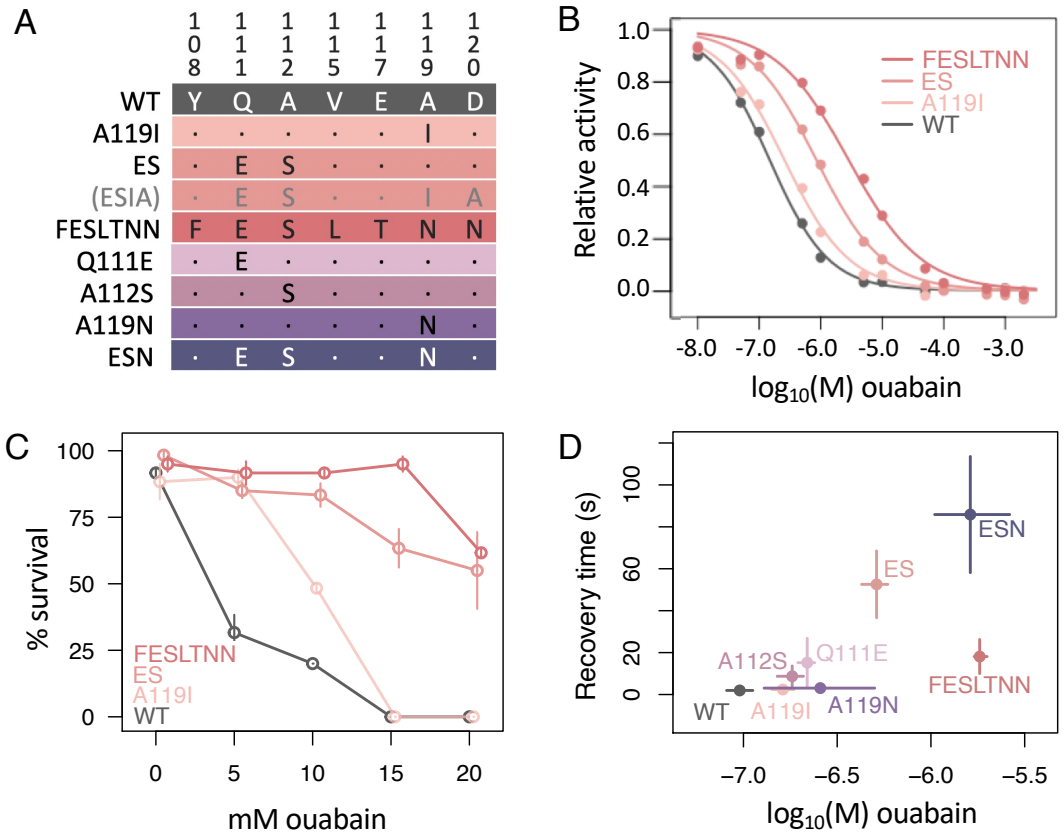

Figure 3. Functional effects of *Photuris* paralog-specific substitutions. (A) Engineered fly lines generated in this study. Only sites implicated in CTS-resistance are shown. States for the CTS-sensitive *D. melanogaster* strain (w^{1118}) used to generate engineered lines are denoted "WT" for "wild-type". Each of the next three lines in increasingly darker shades of red carries a subset of substitutions specific to ATPα1 paralogs A-C. Results for a number of other engineered lines can be found in **Supplementary Figures S4-S6.** (B) CTS-inhibition assays for NKA isolated from heads of WT and engineered fly lines. Mean relative activities (filled circles) are plotted as a function of increasing concentrations of the CTS ouabain. Each mean is the average of three biological replicates (see Methods). Solid lines represent the least squares fit model (see Methods) as in Figure 1. (C) CTS-tolerance of wild-type and engineered adult flies. Survival of adult flies upon seven days exposure to increasing concentrations of CTS (0, 5, 10, 15, 20 mM ouabain). Points represent the average of three biological replicates (n=20 individuals each), and whiskers correspond to standard errors. (D) Levels of neural dysfunction and enzyme resistance to the CTS ouabain for wild-type (WT) and engineered fly lines. The neural dysfunction assay (y-axis) measures the recovery time following seizures induced by mechanical overstimulation (aka "bang sensitivity" assay) of 14-day old male flies (times are capped at 120 seconds). 28-43 individuals (open circles) are assayed for each line, and the mean and 95% bootstrap confidence bounds are indicated as points and whiskers, respectively. The level of enzyme resistance to CTS (x-axis) is measured as IC50 in an ouabain-inhibition assay (see Methods). Plotted is the mean IC50 of three biological replicates (each the average of three technical replicates) and a 95% confidence interval for the estimate.

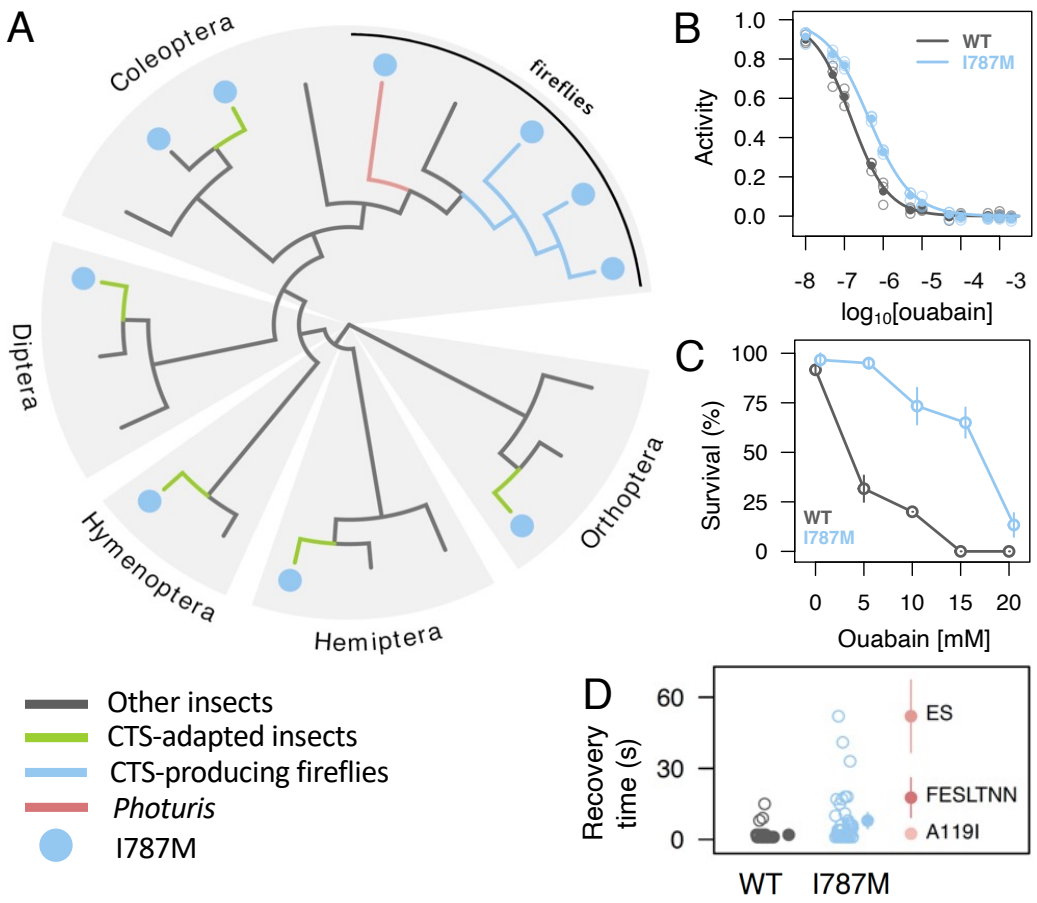

Figure 4. Evolutionary and functional analysis reveals a new CTS-resistance substitution, I787M. (A) Recurrent appearance of I787M in CTS-associated herbivores (green lineages), CTS-producing prey fireflies (blue lineages) and predatory *Photuris* fireflies (red lineage). See **Supplementary Figure S6** for more details. (B) Estimates of the IC50 of NKA of wild-type and engineered fly lines in CTS-inhibition assays. The $\log_{10}(IC_{50})$ of I787M flies (-6.37, 95% CI: -6.39, -6.36) is 2.9-fold higher than that of WT (w^{1118}) control flies (-6.83, 95% CI: -6.87, -6.80). Each estimate is based on three biological replicates (each with three technical replicates). (C) CTS-tolerance of adult wild-type and engineered flies. Engineered flies carrying I787M exhibit higher survival rates upon seven-day CTS exposure. (D) Neural dysfunction as measured by the "bang sensitivity" assay. The assay measures the time to recovery from seizures induced by mechanical over-stimulation (as in **Figure 3**). Open circles correspond to individual flies. Filled circles to the right are means with 95% CI whiskers. I787M individuals are somewhat more susceptible to mechanical over-stimulation than WT (Wilcoxon test p= 3.4e-5), but the impairment is less severe than observed for some other engineered strains. See **Figure 3** for genotypes of A119I, ES, FESLTNN.

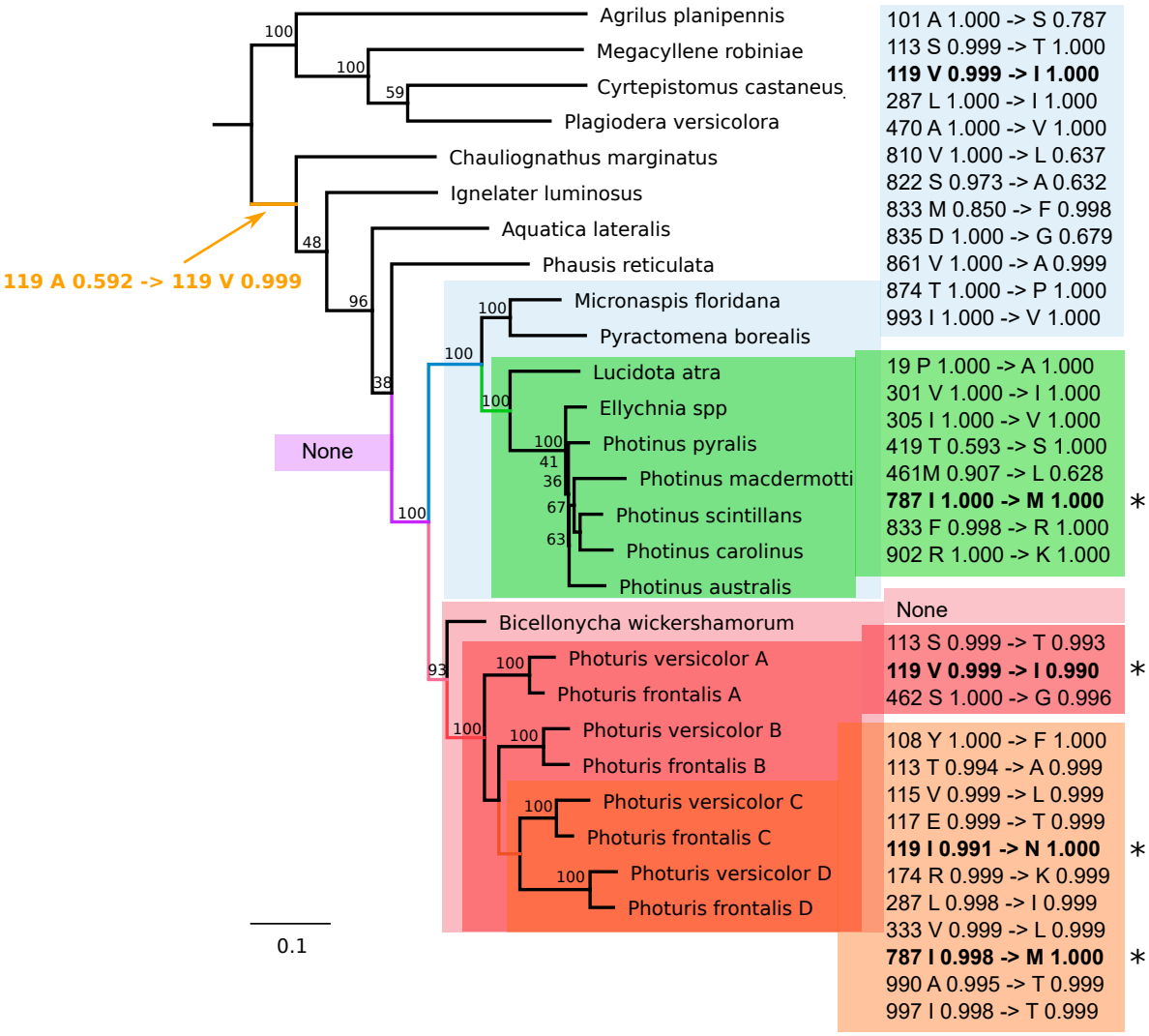

Supplementary Figure S1. **Maximum likelihood (ML) phylogeny with posterior probabilities on amino acid states.** Estimation of the ML phylogeny and ancestral reconstruction implemented in PAML (Yang (1997; see Methods). Numbers on nodes indicate the level of bootstrap support for that particular node. A key finding is that the substitution A119V (in bold orange) evolved prior to the diversification of predatory and prey genera whereas V119I and I787M (asterisks) evolved convergently these genera.

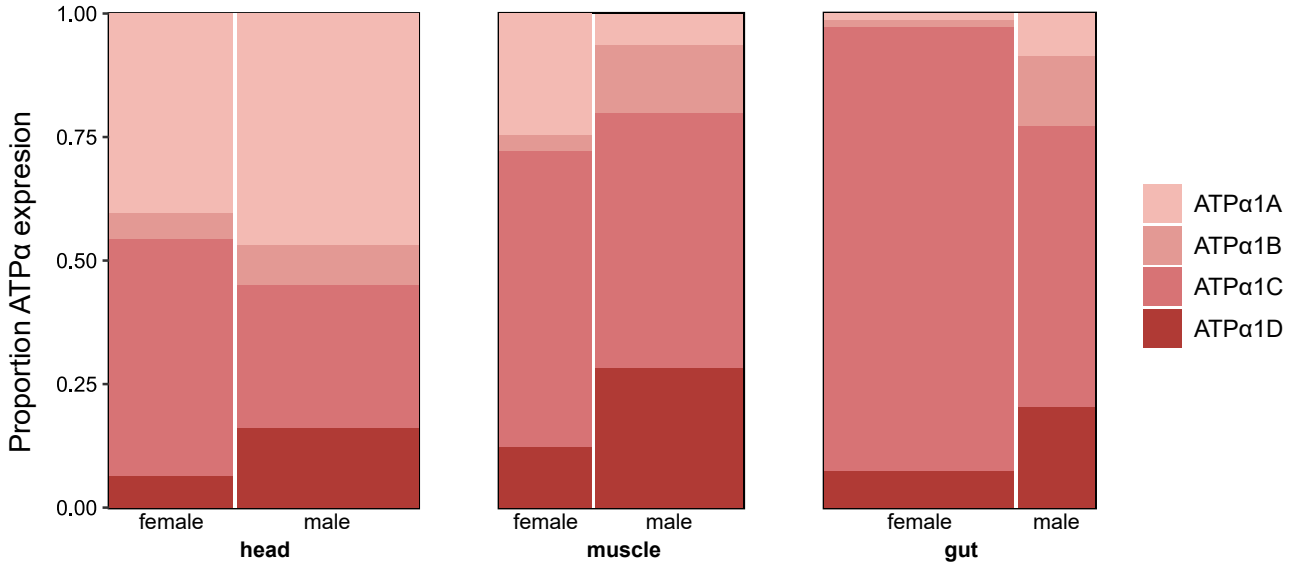

Supplementary Figure S2. Tissue-specific expression of ATPα1 paralogs in *Photuris versicolor* females and males. Column width corresponds to relative proportion of total normalized ATPα1 expression for each tissue summed across paralogs. Shaded segments correspond to relative levels of normalized expression of the four ATPα1 paralogs within each tissue.

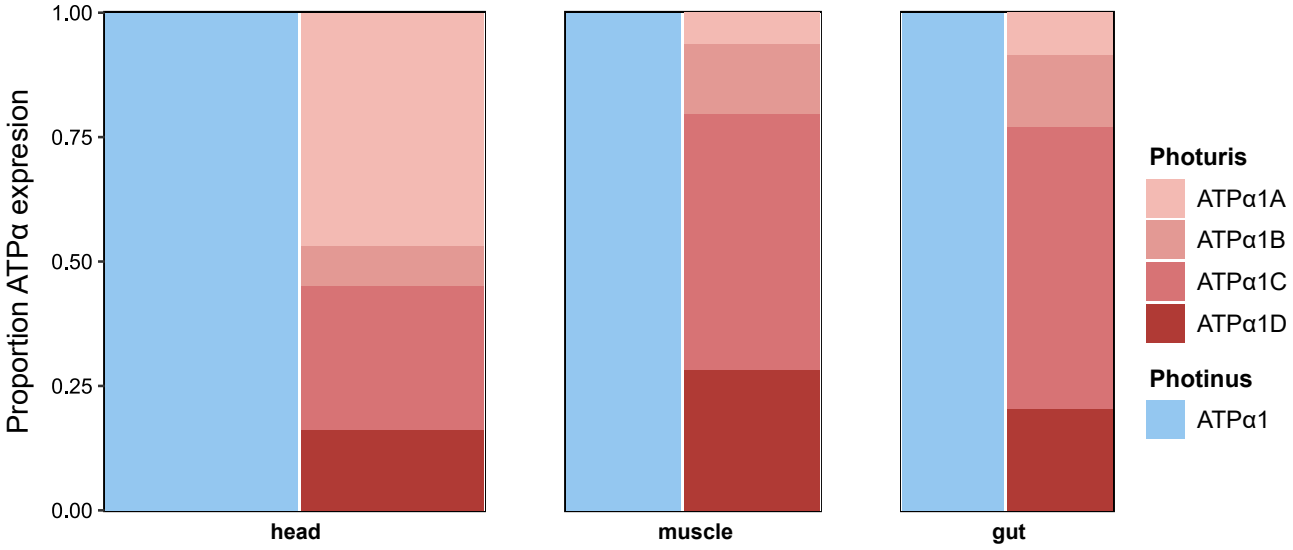

Supplementary Figure S3. **Tissue-specific expression of ATPα1 paralogs in male *Photinus pyralis* (blue) vs *Photuris versicolor* (red) males.** Column width corresponds to relative proportion of total normalized ATPα1 expression across tissues (summed across paralogs in *Photuris*). Shaded segments for *Photuris* correspond to relative and is levels of expression of the four ATPα1 paralogs within each tissue.

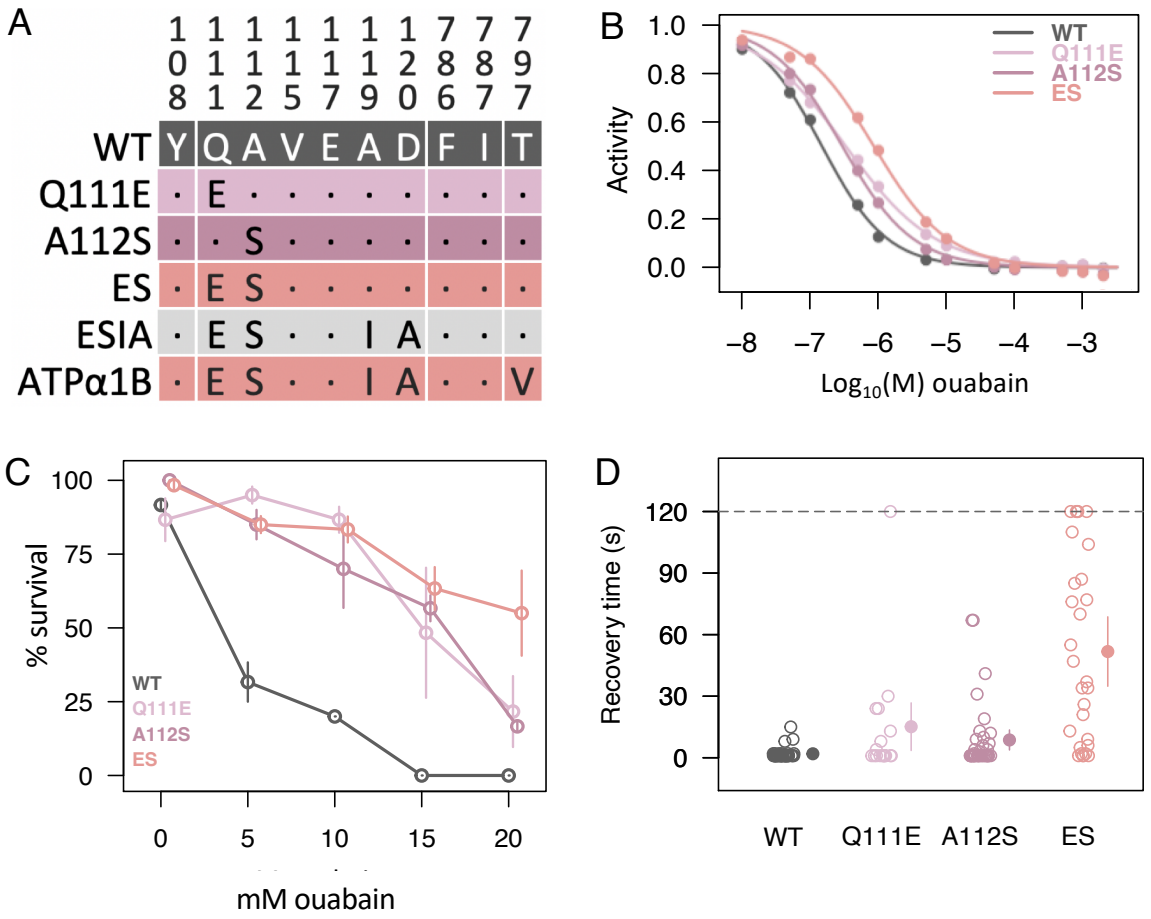

Supplementary Figure S4. Evaluation of intermediate steps in ATPα1B evolution in *Photuris*. **(A)** Engineered fly lines carrying ATPα1B-associated substitutions, individually and in combination. Note that ESIA is homozygous lethal and was not assayed further. **(B)** CTS-inhibition assays for NKA isolated from heads of "wild type" (WT, line w^{1118}) and engineered fly lines (see panel A). Mean relative activities (filled circles) are plotted as a function of increasing concentrations of the CTS ouabain. Each biological replicate (n=3, not shown) is the average of three technical replicates. Solid lines represent the least squares fit model (see **Methods**) **(C)** CTS-tolerance of adult flies. Survival of adult flies upon seven days exposure to different concentrations of CTS (0, 5, 10, 15, 20 mM ouabain). Points represent the average of three biological replicates, and bars correspond to standard errors. **(D)** Level of neural dysfunction. The assay measures recovery times following seizures induced by mechanical overstimulation (aka the "bang sensitivity" assay) of 14-day old male flies Times are capped at 120 seconds. 28-43 individuals (open circles) are assayed for each line, and the mean and 95% confidence bounds (estimated by re-sampling) are indicated as points and whiskers, respectively.

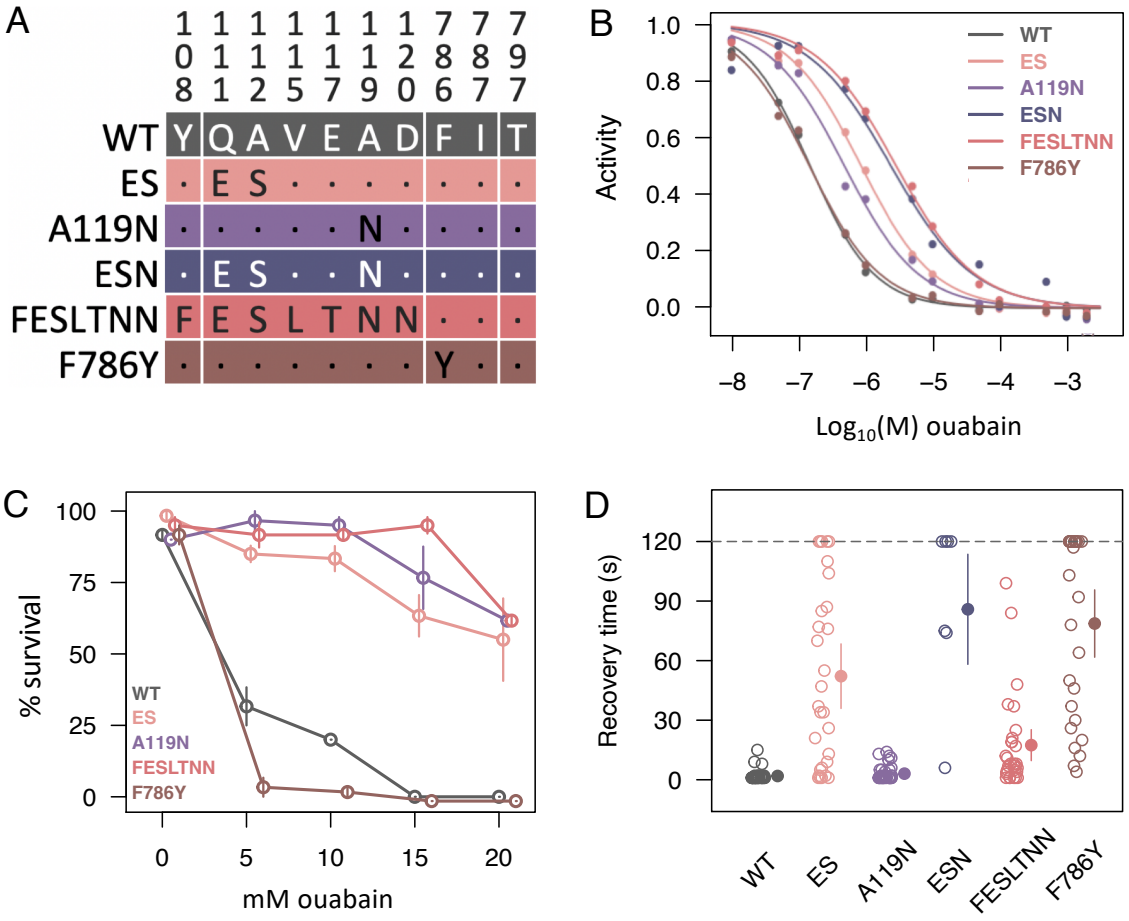

Supplementary Figure S5. Evaluation of amino acid substitutions contributing to CTS resistance of ATPα1 paralogs C and D in *Photuris*. (A) A collection of engineered fly lines carrying ATPα1B substitutions. The color code follows that in the main text. **(B)** CTS-inhibition assays for NKA isolated from heads of w^{1118} (WT) and engineered fly lines. Mean relative activities (filled circles) are plotted as a function of increasing concentrations of the CTS ouabain. Each biological replicate (n=3, not shown) is the average of three technical replicates. Solid lines represent the least squares fit model (see **Methods**) **(C)** CTS-tolerance of adult flies. Survival of adult flies upon seven days exposure to different concentrations of CTS (0, 5, 10, 15, 20 mM ouabain). Points represent the average of three biological replicates, and bars correspond to standard errors. **(D)** Level of neural dysfunction. The assay measures recovery times following seizures induced by mechanical overstimulation (aka "bang sensitivity" assay) of 14-day old male flies (times capped at 120 seconds). 28-43 individuals (open circles) are assayed for each line, and the mean and 95% confidence bounds (estimated by re-sampling) are indicated as points and whiskers, respectively.

Reference	111 Q	112 A	115 V	117 E	119 A	120 D	122 N	786 F	787 I	797 T
Orthoptera										
Tetrix japonica	.	.	.	.	.	.	.	.	.	.
Zonocerus elegans	L	.	.	.	S	.	.	.	.	.
Phymateus leprosus B	L	.	.	.	S	.	.	.	.	.
Phymateus leprosus A	L	.	T	.	T	E	H	.	M	.
Hemiptera										
Lygus hesperus	.	.	.	.	.	.	.	.	.	.
Boisea trivittata	.	.	.	.	S	.	.	.	.	.
Oncopeltus fasciatus D	.	.	.	.	S	.	H	.	.	.
Oncopeltus fasciatus C	.	.	.	.	S	.	H	.	M	S
Oncopeltus fasciatus B	T	S	E	.	S	.	H	N	V	.
Oncopeltus fasciatus A	T	S	.	.	S	.	H	N	V	A
Hymenoptera										
Apis mellifera	.	.	S	D	N	.	.	.	.	.
Monophadnus latus	T	.	L	.	N	.	H	.	M	.
Coleoptera										
Chauliognathus marginatus	.	.	.	.	V	.	.	.	.	.
Photuris versicolor A	.	.	.	.	I	.	.	.	.	.
Photuris versicolor B	E	S	.	.	I	A	.	.	.	V
Photuris versicolor C	E	S	L	T	N	N	.	.	M	I
Photuris versicolor D	E	T	L	T	N	N	.	Y	M	I
Pyractomena borealis	.	.	.	.	I	.	.	.	.	.
Lucidota atra	.	.	.	.	I	.	.	.	M	.
Photinus pyralis	.	.	.	.	I	.	.	.	M	.
Ellychnia spp	.	.	.	.	I	.	.	.	M	.
Tribolium castaneum	.	.	.	.	.	.	.	.	.	.
Chrysochus asclepiadeus	L	.	.	.	S	.	.	.	M	.
Chrysochus auratus A	L	.	.	.	S	.	.	.	.	.
Chrysochus auratus B	V	V	.	.	S	.	H	.	M	.
Diptera										
Drosophila melanogaster	.	.	S	.	.	.	.	.	.	.
Phytomyza fallaciosa	.	.	S	.	S	.	.	.	.	.
Phytomyza hellebori A	H	.	S	.	S	.	H	.	M	.
Phytomyza hellebori B	.	.	S	.	S	.	.	.	M	.

Supplementary Figure S6. Amino acid states at key sites in ATPα1 of CTS-associated insects and representative outgroups. Amino acid numbering follows the standard numbering scheme based on the sheep (*Ovis ares*) ATP1A1 sequence (see Zhen et al. 2012). CTS-associated insects are highlighted in red. The substitution I787M (at highlighted site 787) appears repeatedly in CTS-associated taxa.

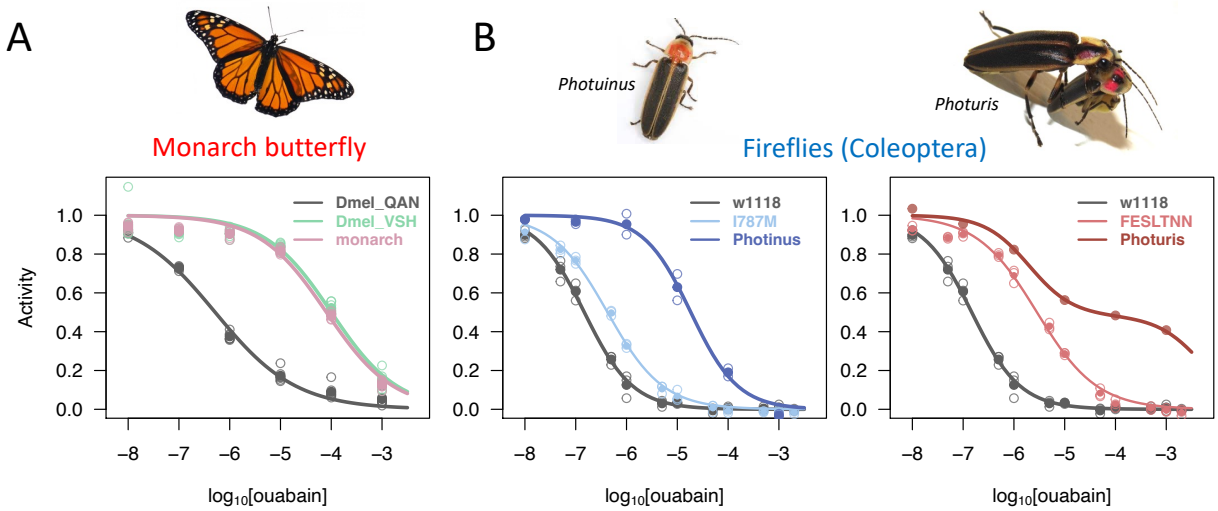

Supplementary Figure S7. CTS-inhibition curves suggest as yet unmapped determinants of CTS resistance in firefly Na^+,K^+-ATPases. (A) Engineering three known CTS resistance-associated amino acid substitutions into *D. melanogaster* Na^+,K^+-ATPAse accounts for ~100% of the CTS resistance of the Monarch butterfly protein (data from Karageorgi et al. 2019). Plots are as in **Figure 1** of main text. Dmel_QAN = wild type *D. melanogaster* protein; Dmel_VSH = *D. melanogaster* protein + substitutions Q111V, A119S and N122H; monarch = Monarch butterfly (*Danaus plexippus*) protein. In contrast, engineering the known major CTS resistance substitutions observed in fireflies into *D. melanogaster* Na,K-ATPase results in only a fraction of the observed CTS resistance of the *Photinus* (left panel) and *Photuris* (right panel) proteins. The latter pattern points to as yet unmapped determinants of CTS resistance of firefly Na,K-ATPases. w1118 = wild-type *D. melanogaster*. The I787M and FESLTNN constructs are described in **Figures 4 and 3**, respectively. "Photinus" and "Photuris" are as in **Figure 1**.

Supplementary Tables

Table S1. Sources of sequence data used in this study.

Species	Collection information	Source
Agrilus planipennis	Lord et al, 2016	XM_018472182.2
Chauliognathus marginatus	this study	ATPα1: MT897473.1
Ignelater luminosus	Fallon et al 2018	Genome: Ilumi1.3, www.fireflybase.org
Aquatica lateralis	Fallon et al 2018	Genome: Alat1.4, www.fireflybase.org
Phausis reticulata	Sander and Hall 2015	RNA-seq: SRR2103663
Bicellonycha wickershamorum	Martin et al 2015	RNA-seq: obtained from the authors
Photuris versicolor	this study	RNA-seq: PRJNA891306, PRJNA922528 ATPα1A: MT897474.1 ATPα1B: MT897475.1 ATPα1C: MT897476.1 ATPα1D: MT897477.1
Photuris frontalis	Sander and Hall 2015; this study	RNA-seq: SRR2104391 ATPα1A: MT897478.1 ATPα1B: MT897479.1 ATPα1C: MT897480.1 ATPα1D: MT897481.1
Micronaspis floridana	Martin et al 2015	RNA-seq: obtained from the authors
Pyractomena borealis	Sander and Hall 2015	RNA-seq: SRR2104393
Pyractomena dispersa	Martin et al 2015	RNA-seq: obtained from the authors
Lucidota atra	Sander and Hall, 2015	RNA-seq: SRR2103572
Photinus pyralis	Fallon et al 2018; this study	Genome: Ppyr1.4, www.fireflybase.org ATPα1: MT897482.1 RNA-seq: PRJNA891248
Ellychnia spp	Martin et al 2015	RNA-seq: obtained from the authors
Photinus australis	Sander and Hall, 2015	RNA-seq: SRR2103451
Photinus macdermotti	Sander and Hall, 2015	RNAseq: SRR2103844

Photinus scintillans	Sander and Hall 2015	RNAseq: SRR2104146
Photinus carolinus	Sander and Hall, 2015	RNAseq: SRR2103825
Megacyllene robiniae	Zhen et al, 2012	ATPα1: JQ771517
Cyrtepistomus castaneus	Zhen et al, 2012	ATPα1: JQ771502
Plagiodera versicolora	Zhen et al, 2012	ATPα1: JQ771522

References

Fallon, Timothy R, Sarah E Lower, Ching-Ho Chang, Manabu Bessho-Uehara, Gavin J Martin, Adam J Bewick, Megan Behringer, et al. "Firefly Genomes Illuminate Parallel Origins of Bioluminescence in Beetles." *ELife* 7: e36495.

Lord, Nathan P., Rebecca L. Plimpton, Camilla R. Sharkey, Anton Suvorov, Jonathan P. Lelito, Barry M. Willardson, and Seth M. Bybee. "A Cure for the Blues: Opsin Duplication and Subfunctionalization for Short-Wavelength Sensitivity in Jewel Beetles (Coleoptera: Buprestidae)." *BMC Evolutionary Biology* 16: 107.

Martin, Gavin J., Nathan P. Lord, Marc A. Branham, and Seth M. Bybee. "Review of the Firefly Visual System (Coleoptera: Lampyridae) and Evolution of the Opsin Genes Underlying Color Vision." *Organisms Diversity & Evolution* 15: 513–26.

Zhen, Ying, Matthew L Aardema, Edgar M Medina, Molly Schumer, and Peter Andolfatto. "Parallel Molecular Evolution in an Herbivore Community." *Science* 337 (2012): 1634–37.

Table S2. Differential expression of ATPα1 paralogs among tissues in *Photuris*.

	P-value	Bonferroni **corrected p-value**	**Fold change**
Among tissues, total ATPα1			
gut ~ head	0.020	0.059	-2.017
gut ~ muscle	3.46E-07	1.04E-06	-11.32
muscle ~ head	5.68E-04	0.0017	5.29
Among tissues by paralog			
ATPα1A			
gut ~ head	1.24E-07	3.73E-07	20.55
gut ~ muscle	0.038	0.11	2.95
muscle ~ head	8.88E-05	2.66E-04	8.52
ATPα1B			
gut ~ head	0.18	0.54	1.92
gut ~ muscle	0.012	0.037	-4.35
muscle ~ head	4.54E-05	1.36E-04	9.65
ATPα1C			
gut ~ head	4.99E-05	1.50E-04	-3.85
gut ~ muscle	6.18E-08	1.85E-07	-15.62
muscle ~ head	8.24E-04	0.0025	4.84
ATPα1D			
gut ~ head	0.23	0.69	-1.77
gut ~ muscle	0.0025	0.0075	-4.93
muscle ~ head	0.010	0.031	-3.31

NOTE - The significance of expression differences was evaluated using raw counts and the IBB tests (Pham and Jimenez, 2012). Corrected P-values apply the Bonferroni correction applied.

References

Pham, Thang V., and Connie R. Jimenez. "An Accurate Paired Sample Test for Count Data." *Bioinformatics* 28, i596-i602.

Table S3. Reagents used for CRISPR-mediated mutagenesis of Drosophila ATPα.

Method 1: Homology dependent repair (HDR) using one guide RNA and a dsDNA plasmid donor **Lines: A119I (Line A); Y108F-Q111E-A112S-S115L-E117T-A119N-D120N (Line C); Q111E-A112S-A119I-D120A (homozygous lethal)**	
gRNA target site [PAM]	gRNA1: 5'-CTTTGTGGCCTATTCTATCC[AGG]-3' (plus strand) gRNA2: 5'-GGTGCTGGCCTGGATAGAAT[AGG]-3 (minus strand) gRNA3: 5'-GGCCGACGATAATTTGTATC[TGG]-3' (plus strand)
Synonymous PAM mutations	gRNA1: CAG (Q) →CAA (Q) gRNA2: GCC (A) →GCG (A) gRNA3: CTG (L) → CTC (L)
Homology arms	Upstream: 1069bp,3R: 20963017-20964085 Forward primer: 5'-CAAAGGCTTTCGAGGTCAGCG Reverse primer: 5'-GGCCACAAAGCAGAGAATAGCAC Downstream: 1066bp,3R: 20964154-20965219 Forward primer: 5'-CGCTGTCGTCATCGTGACGGGCATTTT Reverse primer: 5'-CGAATGTTCATCACATCGCCC
Line: T797I (homozygous lethal)	
gRNA target site [PAM]	5'-GTGGCAGTGGTATATCGCAG[AGG]-3' (minus strand)
Synonymous PAM mutation	ATC (I) → ATT (I)
Homology arms	Upstream: 1082bp, 3R: 20965493-20966574 Forward primer: 5'-CGACAAGTATCCCAACGGCT Reverse primer: 5'-TCCCAGTGGCAGTGGTATATCG Downstream: 1059bp, 3R: 20966660-20967718 Forward primer: 5'-AGTTAAAGTTGCTATTAAGTCAGTAT CATTCGAGCAA Reverse primer: 5'-GGGAGCGGTTATATGAGCGTA
Method 2: One guide RNA and ssODN **Lines: F786Y and I787M (Line P)**	
gRNA target site [PAM]	5'-TGGTATATCGCAGAGGATGA[AGG]-3' (plus strand)

gRNA primers	Forward primer: 5’-GAAATTAATACGACTCACTATAGGTGGTATATCGCA GAGGATGAGTTTTAGAGCTAGAAATAGC-3’ Reverse primer: 5’-AAAAGCACCGACTCGGTGCCACTTTTTCAAGTTGAT AACGGACTAGCCTTATTTTAACTTGCTATTTCT AGCTCTAAAAC-3’
ssODN for F786Y	5’-GGAGGAGGGTCGCCTGATCTTCGACAACCTGAAAAA GTCCATCGCCTACACCCTGACCTCCAACATTCCCGAAATCTCGCCCTTC CTGGCCTatATtCTgTGCGATATACCACTGCCACTGGGAACCGTGACGAT T-3’ (Letters in lower case represent substitutions. Underlined codon is the target of interest. “Tat” substitutes F to Y.)
ssODN for I787M	5’-TGTGGAGGAGGGTCGCCTGATCTTCGACAACCTGAA AAAGTCCATCGCCTACACCCTGACCTCCAACATTCCCGAAATCTCGCC CTTCCTGGCgTTCATgCTgTGCGATATACCACTGCCACTGGGAACCGTG ACGATT-3’ (Letters in lower case represent substitutions. Underlined codon is the target of interest. “ATg” substitutes I to M.)
primers for amplicon sequencing	Forward primer: 5'-TCGTCGGCAGCGTCAGATGTGTATAAGAGACAGCCC TGACCTCCAACATTCCC-3' Reverse primer: 5'-GTCTCGTGGGCTCGGAGATGTGTATAAGAGACAGGT CAGCCGCACAATTTANGT-3' (Underlined region is complementary to template DNA primer.)

NOTE – coordinates correspond to the *D. melanogaster* genome reference release=r6.49 (http://flybase.org)

Table S4. Estimates of CTS-resistance of Na,K-ATPase (IC_{50} of ouabain).

Drosophila lines	$log_{10}(IC_{50})$	$log_{10}(IC_{50})$ 95% Confidence Intervals	Fold-change (relative to Dmel w^{1118})	Hill slope (hs)	hs 95% Confidence Intervals
"WT" Drosophila strains					
Dmel (w^{1118})	-6.83	-6.89, -6.77	-	-0.91	-1.03, -0.82
Dmel (Oregon R)	-6.83	-6.88, -6.78	1.0	-0.94	-1.06, 0.84
Dmel (GE-WT)	-6.80	-6.83, -6.77	1.1	-0.95	-1.04, -0.88
Engineered Drosophila strains					
A119I	-6.59	-6.62, -6.56	1.8	-0.83	-0.89, -0.77
Q111E	-6.48	-6.52, -6.45	2.2	-0.66	-0.71, -0.62
A112S	-6.53	-6.56, -6.51	1.9	-0.84	-0.91, -0.78
A119N	-6.32	-6.40, -6.23	3.0	-0.79	-0.87, -0.73
ES	-6.07	-6.10, -6.04	6.0	-0.80	-0.86, -0.75
ESN	-5.63	-5.66, -5.58	16	-0.70	-0.86, -0.55
FESLTNN	-5.52	-5.56, -5.53	18	-0.73	-0.77, -0.70
F786Y	-6.84	-6.87, -6.81	0.93	-0.82	-0.88, -0.76
I787M	-6.37	-6.39, -6.36	2.9	-0.79	-0.84, -0.75
Wild-caught fireflies					
Photinus	-4.73	-4.87, -4.61	125	-0.95	-1.09, -0.81
Photuris					
Biphasic model	-5.73 -2.27	-5.87, -5.60 -2.44, -2.00	13 3.6e4	(1)	-
Monophasic model	-5.50	-5.65, -5.33	22	-0.73	-0.96, -0.54

Note: 95% confidence intervals on IC_{50} were estimated by bootstrap simulation, see Methods.

Dmel = "wild-type" *D. melanogaster*, represented by strains w^{1118} (the strain used to engineer substitutions using CRISPR-cas9), GE-WT (the strain used for the engineering method of Taverner et al. (2019)) and "Oregon R" a standard lab strain. The estimate for GE-WT was estimated from the data of Taverner et al. (2019). Note that *Photuris* IC_{50} are estimated under two alternative models and several simplifying assumptions (see Methods). Notably the biphasic model assumes that there are two forms of the enzyme with distinct IC_{50}, the Hill-slope (hs) is 1 and the activity of the enzyme under maximum inhibition is 0. The monophasic model assumes that there is one form of the enzyme and activity of the enzyme under maximum inhibition is 0.4.

References

Taverner, Andrew M, Lu Yang, Zachary J Barile, Becky Lin, Julie Peng, Ana P Pinharanda, Arya S Rao, et al. "Adaptive Substitutions Underlying Cardiac Glycoside Insensitivity in Insects Exhibit Epistasis in Vivo." *ELife* 8: e48224.